Evaluation of Laboratory Cracking Tests Related to Top-Down Cracking in Asphalt Pavements

by

Nathan D. Moore

A thesis submitted to the Graduate Faculty of
Auburn University
in partial fulfillment of the
requirements for the Degree of
Master of Science

Auburn, Alabama
December 10, 2016

Keywords: Asphalt, Top-down cracking, Laboratory cracking tests

Approved by

David H. Timm, Chair, Brasfield & Gorrie Professor of Civil Engineering
Randy C. West, Director of the National Center for Asphalt Technology
Jeffrey J. LaMondia, Associate Professor of Civil Engineering

ABSTRACT

Top-down cracking (TDC) is now recognized as a prominent mode of failure in asphalt pavements. There has been much research conducted to characterize the failure mechanisms of TDC but there are still large gaps of knowledge regarding TDC throughout the industry. As TDC causes premature failure and costly, unplanned maintenance, there is need for a screening tool that would predict TDC susceptibility in asphalt pavements during design.

The objective of this thesis is to evaluate seven surface mixtures with a wide range of properties yielding mixtures that span from predictably TDC susceptible to predictably very TDC resistant. This was done by testing the mixtures using five laboratory cracking tests: Energy ratio, Texas Overlay Test, NCAT Overlay Test, Semi-circular Bend Test, and Illinois Flexibility Index Test. The results of the five tests for each mixture were summarized and will be used to compare mixture laboratory performance to mixture field performance to determine which test most accurately predicted field performance.

The results of the study showed that the Energy Ratio produced somewhat predictable results but needs modification to allow for application as a TDC screening tool during design. The SCB and IFIT possessed the lowest variability but produced conflicting results with each other and the expected performance trends. Finally, both Overlay methods exhibited high variability although they most closely followed the expected performance trends. Field performance data are needed to validate any of these findings and will be reported later.

ACKNOWLEDGMENTS

I would like to sincerely thank my advisor and committee chair, Dr. David Timm, for his guidance and assistance during my tenure as a graduate student. He gave me this project knowing that I would enjoy working in the lab and getting my hands dirty. His guidance throughout my studies has been extraordinarily gracious and encouraging. Even beyond assisting me for the purpose of this thesis, Dr. Timm's door was always open, and he was always willing to give advice regarding anything I could ask. From the very first day he set an example of a hard worker with a well-balanced life outside of work. He never asked his students to do any menial or difficult task that he was not willing to do himself. His demonstration of excellence was contagious and I am very grateful and honored to have been his student.

Secondly, I would like to thank Dr. Randy West for his leadership and willingness to allow me to participate in this project. His excellent example of a director and researcher inspired me to work hard and to the best of my ability. Allowing me to participate in meetings and conversations that reinforced the purpose, importance, and background for this project helped tremendously during the testing and writing for this thesis.

Next, I would like to thank Dr. Jeffrey LaMondia for his assistance for all my statistical questions during this research. Dr. LaMondia is the reason I chose to pursue a career in research as he taught me by example during my time as an undergraduate student. Through working with Dr. LaMondia, I learned how to participate in the conversation of research as well as how to

write excellently. I am very thankful for his helpfulness and willingness to answer constant questions and concerns.

I would also like to personally thank Adam Taylor for his assistance during this project. His knowledge regarding asphalt laboratory testing is outstanding, and he is responsible for much of what I know about this field of work. He was an exceptional teacher and a very patient colleague. His leadership, as my former boss, is the reason I decided to pursue a Master's degree and a career in asphalt pavements.

This thesis could not have been completed without the incredible work of Tina Ferguson. Her attention to detail is stunning and was critical to this project as she prepared specimens, ran tests, and reported and stored test results in a neatly organized way. I would also like to thank Jason Moore, Brian Waller, Dr. Saeed Maghsoodloo, Vickie Adams, and the many co-op students and lab technicians that assisted me in data collection and reporting throughout this project.

I also wish to thank the Cracking Group experiment sponsors for their cooperation and support of this research. The sponsors include the following departments of transportation: Alabama, Florida, Illinois, Michigan, Minnesota, New York, North Carolina, Oklahoma, South Carolina and Wisconsin. The Alabama Department of Environmental Management and the Federal Highway Administration also sponsored this research.

Finally, I want to thank my wife, Anna Clair. Her support and encouragement was priceless, and I could not have completed this work in the manner I did without her. I am immeasurably grateful for her.

TABLE OF CONTENTS

LIST OF TABLES

LIST OF FIGURES

CHAPTER 1 – INTRODUCTION

1.1 Problem Statement

Top-down cracking (TDC) has been widely reported as a primary mode of distress in asphalt pavements (Hugo & Kennedy, 1985; Myers, et al., 1998; Gerritsen, et al., 1987). Figure 1 displays an example of a pavement core with TDC. Despite the prevalence of TDC there is not a universal consensus regarding the exact causes or mechanisms of TDC among researchers and engineers. Therefore, there is a large gap between the data being acquired and interpreted to address the problem of TDC and the implementation of procedures to mitigate or prevent it.

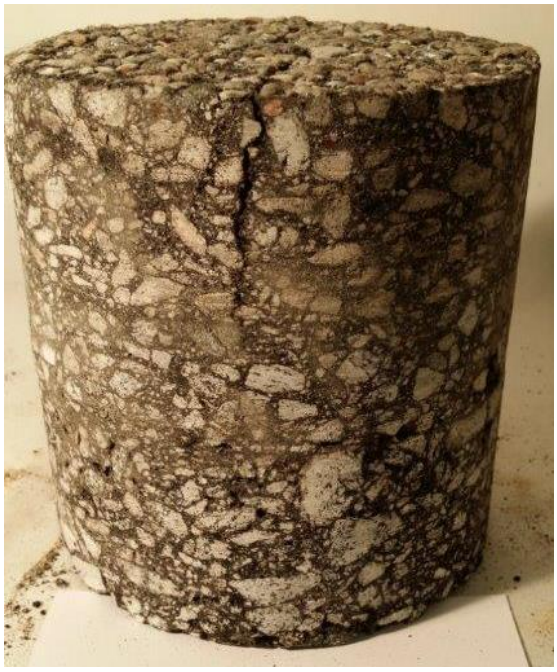

Figure 1: TDC in pavement core.

Most researchers agree that TDC is in some measure caused by high stresses induced by radial tires at the pavement surface; however, a variety of stress types have been proposed as the true failure mode. Gerritsen, et al., (1987) have posited that radial inward shear forces under rubber

truck tires often initiate surface cracks while crack propagation is controlled by thermal stresses induced by changing temperatures. Hugo and Kennedy (1985) reported that high residual stresses from the elastoplastic behavior of asphalt pavements can lead to early fatigue in the surface layers. The high residual stresses are exacerbated by high thermal stresses and age-hardened binder. The idea that age-hardened binder plays a role in TDC seems to be confirmed by Matsuno and Nishizawa (1992). They noticed that TDC often did not occur on sections of pavements directly beneath bridge overpasses, thus avoiding most direct sunlight during daylight. Myers, et al., (1998) studied the effects of tire-induced surface tensile stresses and found that transverse tensile stresses at the tire-pavement interface were the primary failure mode on many pavements experiencing TDC. Many of the pavements in their study had wider cracks at the surface of the pavements than further down into the pavement structure, indicating a tension-controlled opening mode. Myers et al., (1998) also noted that surface tension from radial tires is essentially unaffected by pavement design characteristics and mixture properties. In fact, most of the pavements where TDC was occurring were determined to be otherwise structurally sound.

Although TDC damage is not as severe as bottom-up fatigue cracking and much easier to repair, the costs of milling and inlaying new surface layers is a significant expense. If TDC susceptible mixtures could be screened out during the mixture design process the risk of premature surface failure would be greatly reduced. In 2015, a study at the National Center for Asphalt Technology (NCAT) began with the purpose of gaining more understanding about TDC and to determine a current industry-accepted laboratory cracking test that could accurately predict TDC in asphalt pavements. Seven test mixtures were designed and constructed on the NCAT Test Track with widely varying properties including density, binder type, recycled material type, and recycled

material proportion to cover a wide range of cracking susceptibility. The experiment sponsors chose the types of mixtures that would be used. The mixtures were constructed as surface lifts overlaying highly polymer-modified base and binder layers. This was done to prevent bottom-up fatigue cracking and isolate TDC as the primary mode of potential failure.

Five laboratory cracking tests were selected by the experiment sponsors to be used for this study. The sponsors voted on these five tests based on past experience and testing history. The five tests were the Energy Ratio (ER), Texas Overlay Test (TX-OT), NCAT Modified Overlay Test (NCAT-OT), Semi-circular Bend test (SCB), and the Illinois Flexibility Index Test (IFIT). Each mixture was analyzed using the five cracking tests and the compilation of the results yielded relative rankings for the mixtures in terms of expected cracking resistance. The relative rankings over all five tests will be used to analyze how well the mixtures actually perform with regards to the expected performance. As cracking occurs on the Test Track the results of the study presented in this thesis will be compared to field performance of the seven mixtures.

1.2 Objective and Scope of Work

The objective of this study was to evaluate the TDC susceptibility of seven mixtures currently in place on the NCAT Test Track using the five previously mentioned laboratory tests. In the future, the cracking test results will be used to compare the lab performance of the mixtures with future field performance on the Test Track. Lab-to-field correlations will provide valuable data on the test mixtures and the cracking tests to improve on the current understanding of TDC in the industry and to potentially recommend a cracking test to accurately predict TDC. This thesis contains the results of the plant-mixed, lab-compacted (PMLC) specimens. Future work will

include testing of short and long-term laboratory aged lab-mix, lab-compacted specimens as well as long-term aged PMLC specimens.

1.3 Organization of Thesis

This thesis includes five chapters. This chapter (Chapter 1) contains an explanation of the background and objective of this project. Chapter 2 includes a literature review of the presumed causes and mechanisms of TDC and of the history and implementations of the five previously mentioned cracking tests. The cracking tests' analysis calculations and typical test results are also discussed here. Chapter 3 discusses the methodologies followed for the mixture sampling, cracking tests, and statistical analyses. This chapter also describes the process of the cracking experiment from design of the experimental mixtures to final test result analysis. Chapter 4 includes the results of the cracking tests and the statistical analyses with discussion. The cracking tests' results were analyzed according to each individual test. Mixture result trends across the five tests are noted here as well as general comments regarding the cracking tests. Chapter 5 presents conclusions from the results. The key results are summarized and are compared with the most up to date field performance data. The feasibility of implementation of each of the five cracking tests as a screening tool is also discussed in Chapter 5.

CHAPTER 2 – LITERATURE REVIEW

This section summarizes some of the current literature on the causes and mechanisms of TDC. Also included in this section are descriptions of the history, concepts, and current implementation of the ER, TX-OT, NCAT-OT, SCB, and IFIT.

2.1 Top-Down Cracking

TDC has been a substantial topic of research in the asphalt pavement industry over the past 30 years. In 1985, Hugo and Kennedy reported TDC occurring in South Africa, and two years later Gerritsen, et al. (1987) published one of the first papers regarding how to predict TDC in asphalt pavements using tire-induced radial stresses in the wheelpath. In 1992, Matsuno and Nishizawa believed that TDC was completely independent of pavement structural quality and thickness. In their encounters with TDC they were unable to discriminate between sufficiently performing and poor performing pavements based on pavement structure. They assumed that TDC was caused by tensile strains at the edge of the tire at high temperatures. A finite element method (FEM) analysis confirmed that large tensile strains occurred close to the edge of the tire at high temperatures with the stiffness of the surface layer was relatively low. When binder in the surface course had been age-hardened, the surface cracks tended to not heal under the kneading of the tires. Pavements in direct sunlight were much more brittle than pavements that avoided direct sunlight during the hottest time of day like pavements beneath bridge passes. As expected, TDC was found to be much more prevalent in pavements exposed to direct sunlight compared to pavements beneath bridge passes. Due to these findings, Matsuno and Nishizawa concluded that the combination of aged-hardened pavements with high tensile strains at the tire edge led to TDC.

Although the TDC was thought to have been independent of structure quality by early researchers, this assumption has been contradicted by later studies (Myers, 2000; Uhlmeyer, et al., 2000). In 2010, Roque, et al. reported that TDC has two primary mechanisms that are often present in pavements with TDC:

1) Bending-induced surface tension away from the tire which controlled TDC initiation in pavements with low to moderate thickness.
2) Shear-induced near-surface tension at the edge of the tire which governed crack initiation in thicker pavements.

Typical mechanistic pavement analysis heavily relies on assumptions of uniform wheel loading and single modulus pavement structures. These assumptions are fine for sub-surface stress-strain analysis but cannot capture the effects of temperature depth gradients and tire-pavement interactions (Pellinen, et al., 2004). The idea that pavements are more susceptible to TDC in high temperatures was tested in a lab by de Freitas, et al. in 2005. In a study of accelerated loading of lab-compacted slabs, surface cracks initiated earlier at higher temperatures. Interestingly, they found that FEM stress distributions in pavements with rut depths of 5 mm were greatly increased in the wheel path compared to pavements with no rutting.

As the knowledge gap regarding TDC grows narrower, practitioners have begun to implement strategies to prevent TDC from occurring. Numerous studies showed that TDC was occurring in pavements with segregation, high air voids, low amounts of fines, and aged binder. Therefore methods were introduced to mitigate TDC such as avoiding constructing surface layers with high air void contents, increasing binder content in surface layers, and implementing stringent measures during construction to prevent mixture segregation (de Freitas, et al., 2005; Harmelink,

et al., 2008). Although a deeper understanding of the causes and effects associated with TDC has been achieved, much work is still required to determine if there are any structural reasons for TDC occurrence.

The Mechanistic-Empirical Pavement Design Guide adopted models to assess TDC initiation and propagation in asphalt pavements. Detailed information regarding the development and implementation of these models are discussed in another document (Roque, et al.,, 2010). However, since the implementation of the models proposed by Roque, et al. (2010), it has been reported that the TDC model in the MEPDG fails to predict TDC accurately in the field (Wen & Bhusal, 2015). This problem most likely stems in part from the fact that complex models are required to simulate binder aging to determine an estimate of the effects of binder aging on the pavements (Wang, et al., 2007). Different models or further calibration and validation for this model are needed to be able to assess a wider range of pavements.

Forensic analysis has been accomplished by researchers and engineers to create or improve methods to identify or prevent TDC. As discussed previously, some practitioners have even implemented strategies to mitigate TDC by increasing binder contents and avoiding segregation during construction. However, there is no universally accepted standard or test for practitioners to gauge TDC susceptibility for various mixture designs. This is primarily due to the fact that there is still much left to learn about TDC mechanisms and structural causes. TDC can be an expensive problem for DOTs in regions with significant proportions of pavements failing prematurely due to TDC. Some pavements in Colorado and Washington have had reported TDC as early as one to three years of initial construction (Harmelink, et al., 2008; Uhlmeyer, et al., 2000). Even as structural forensic analysis and modeling continues, there is a need to understand

in greater detail how to predict TDC in the mixture design. Researchers at the University of Florida and the Florida Department of Transportation (FDOT) have made most of the progress on this issue by introducing the Energy Ratio concept to pavement design (Roque, et al., 2004). The Energy Ratio uses a combination of three asphalt mixture performance tests to estimate TDC resistance. This test will be discussed in the next section.

2.2 Energy Ratio

The Energy Ratio (ER) was developed by researchers at the University of Florida to predict asphalt pavement performance with regards to TDC (Roque, et al., 2004). The ER approach was a product of an HMA Fracture Mechanics Model also developed at the University of Florida (Zhang, et al., 2001). In recognition that no single variable in mixture property had been able to accurately and consistently correlate to TDC, Roque, et al. (2004) combined the results of three tests used in the HMA Fracture Mechanics Model to form a more comprehensive measurement of TDC susceptibility. The ER is determined from results of the resilient modulus (ASTM D7369-11), creep compliance (AASHTO T322-07), and indirect tensile strength (ASTM D6931-12), all of which can be performed on the Superpave IDT, at a test temperature of 10 °C. Figure 2 illustrates the main concept of the ER. Dissipated creep strain energy (DCSE) threshold is an intrinsic property of every asphalt mixture at which it will form a microcrack. In other words, the DCSE threshold is the amount of energy required beyond the elastic region of a mixture to initiate cracking. The DCSE threshold is determined by calculating the area under the stress-strain curve and subtracting the estimated resilient modulus, as shown in Figure 2. The energy that is applied to cause a fracture in the pavement is accumulated at a rate governed by the creep compliance parameters, D_1 and m-value, of the mixture. Using the HMA Fracture Mechanics

Model, Roque, et al. (2004) evaluated 36 cores for 22 different mixtures (792 total cores) and determined predicted cycles to failure for the mixtures. The cycles were not representative of wheel passes or ESALs but were instead simulations of tensile stress events in a pavement with given creep compliance parameters and average tensile stress. A value of 6,000 predicted cycles was selected as the failure criterion as it separated mixtures that cracked from those that did not in the field. The DCSE accumulated after 6,000 cycles, or $DCSE_{min}$ is calculated by (Roque et al., 2004) in Equation 1:

$$DCSE_{min} = \frac{m^{2.98} D_1}{0.0299 \times \sigma^{-3.10}(6.36 - S_t) + 2.46 \times 10^{-8}} \quad [1]$$

Where:

m & D_1	=	Creep compliance parameters
σ	=	Tensile stress at bottom of asphalt layer (MPa)
S_t	=	Tensile strength (MPa)

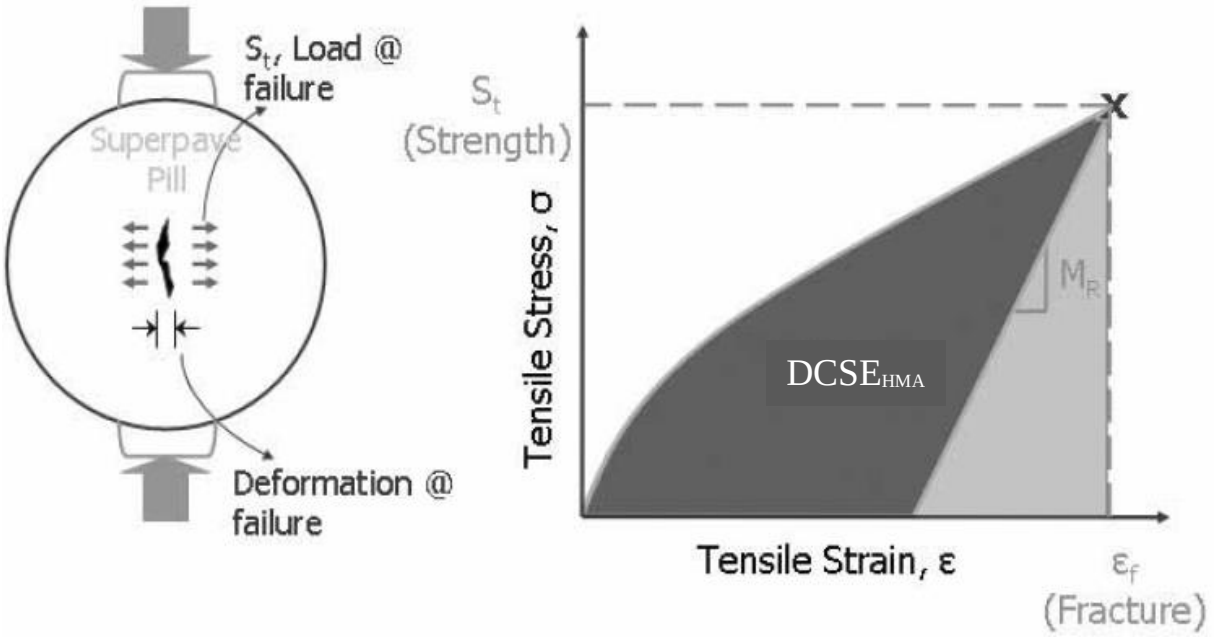

Figure 2: DSCE threshold concept (After Roque, et al., 2004).

The energy ratio is the ratio between the dissipated creep strain energy threshold of the mixture, $DCSE_{HMA}$, shown in Figure 2, and the minimum dissipated creep strain energy required to resist TDC. This equation is listed below as Equation 2. A mixture with an ER of greater than 1.0 would be considered acceptable.

$$ER = \frac{DCSE_{HMA}}{DCSE_{Min}} \quad [2]$$

Where:

ER	=	Energy Ratio
$DCSE_{HMA}$	=	Dissipated Creep Strain Energy Threshold
$DCSE_{Min}$	=	Minimum required Dissipated Creep Strain Energy

The ER accurately separated cracked and uncracked sections in 19 of the 22 pavements studied in Florida (Roque, et al., 2004). Additional parameters were recommended to supplement the ER criteria for the sections that did not match their predicted performance. Mixtures from two sections yielded energy ratios of greater than 1.0 but still exhibited TDC. Both sections had $DCSE_{HMA}$ thresholds less than 0.75 kJ/m^3 while an uncracked mixture that had an ER of less than 1.0 had a $DCSE_{HMA}$ threshold of 2.5 kJ/m^3. Therefore, an additional parameter based on the $DCSE_{HMA}$ value was added to screen out very stiff and brittle mixtures. Table 1 shows the ER criteria published by Roque, et al. (2004) for mixtures with different traffic applications and the supplemental criteria based on the $DCSE_{HMA}$.

Table 1: Energy Ratio Criteria.

Mix Property	Criterion	
Energy Ratio	Traffic ESALs (x1000):	Min. Energy Ratio
	<250	1.0
	<500	1.3
	<1,000	1.95
$DCSE_{HMA}$	> 0.75 kJ/m^3	
$DCSE_{HMA}$	Recommended Range: 0.75 – 2.5 kJ/m^3	

The ER has been applied to other pavements using field cores, lab testing, and M-E design (Shu, et al., 2008; Timm, et al., 2009; Willis, et al., 2009; Wang, et al., 2007; Willis, et al., 2016). FDOT sponsored research to refine the procedure for mixture approval with regards to TDC susceptibility, but at the time the equipment required was too complex to fully implement such a procedure (Willis, et al., 2009). Willis, et al. (2016) used the ER to assess mixtures with a variety of sustainable materials and properties. A GTR mixture was the first to crack, but the crack propogation rate of the GTR mix was slow. A mixture with 20% RAP, 5% RAS, and SBS-modified binder exhibited the highest ER but failed to meet the minimum $DCSE_{HMA}$ criteria. This mixture cracked quickly and had an extremely rapid rate of crack growth. A mixture with 25% RAP and SBS-modified binder cracked sooner and faster than a virgin mixture with SBS-modified binder due to the extra stiffness from the combination of RAP and SBS and failed to exceed the minimum $DCSE_{HMA}$ threshold. Timm, et al. (2009) compared the ER results of two pavements with similar aggregate structure and in-place denisty but one pavement had unmodifed PG 67-22 binder and the other had polymer-modified PG 76-22 binder. The section with PG-76-22 binder outperformed the section with PG 67-22 binder in ER results and field

performance.

2.3 Texas Overlay Test

The Texas Overlay Test (TX-OT) was originally developed in the late 1970's to simulate reflective cracking of asphalt overlays on concrete pavements, and the method was refined in the 2000's by Zhou and Scullion (2005). The test was adapted for the Asphalt Mixture Performance Tester (AMPT) by one equipment manufacturer (IPC Global, 2012). Overlay Test specimens are cut from a SGC sample or a field core and glued to two metal plates with a 4.2 mm gap between them, shown in Figure 3. One plate remains fixed while the other plate moves in a displacement controlled mode while applying a sawtooth wave load to a maximum opening displacement (MOD) once per 10 second cycle (5 second of loading, 5 for unloading) (Figure 4). Testing is performed at 25 °C with a maximum opening displacement of 0.635 mm in according to the test specification, Tex-248-F. Therefore, in one cycle the plates begin at 4.2 mm apart and open to 4.835 mm before returning to 4.2 mm at the completion of the cycle. The maximum opening displacement simulates the expansion and contraction that occurs at the joints of portland cement concrete pavements due to temperature fluctuation. The peak load on the first cycle is measured and the test reaches failure when a cycle registers a load that is a 93% reduction of the initial peak load and the number of cycles to failure (N_f) is recorded.

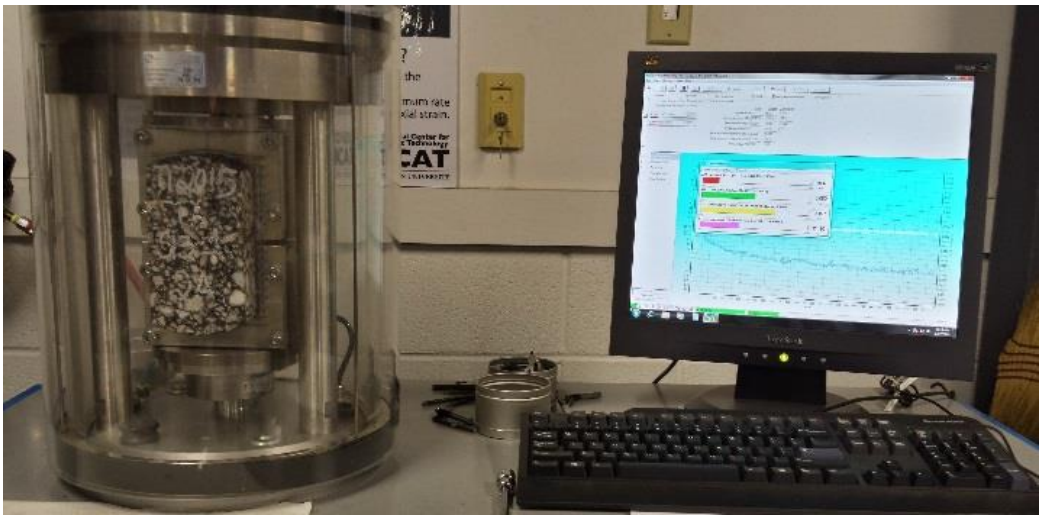

Figure 3. Overlay Test setup on AMPT.

Zhou and Scullion (2005) initially demonstrated that the OT is sensitive to testing temperature, maximum opening displacement, and asphalt binder content and type. A more in-depth sensitivity study was performed by Walubita et al. (2012) that reviewed the current state of the OT in a number of labs in the United States. High variability (CV > 30%) was reported in many of the labs. Walubita, et al. (2012) assumed that a significant proportion of the variability was due to either poor provisional OT specifications or poor adherence to Tex-248-F. Even when strict adherence to Tex-248-F was present, the inherent variability that arises from cyclic fatigue testing was still present. It was recommended that four or five specimens be tested and that the middle three results reported (Walubita, et al., 2012).

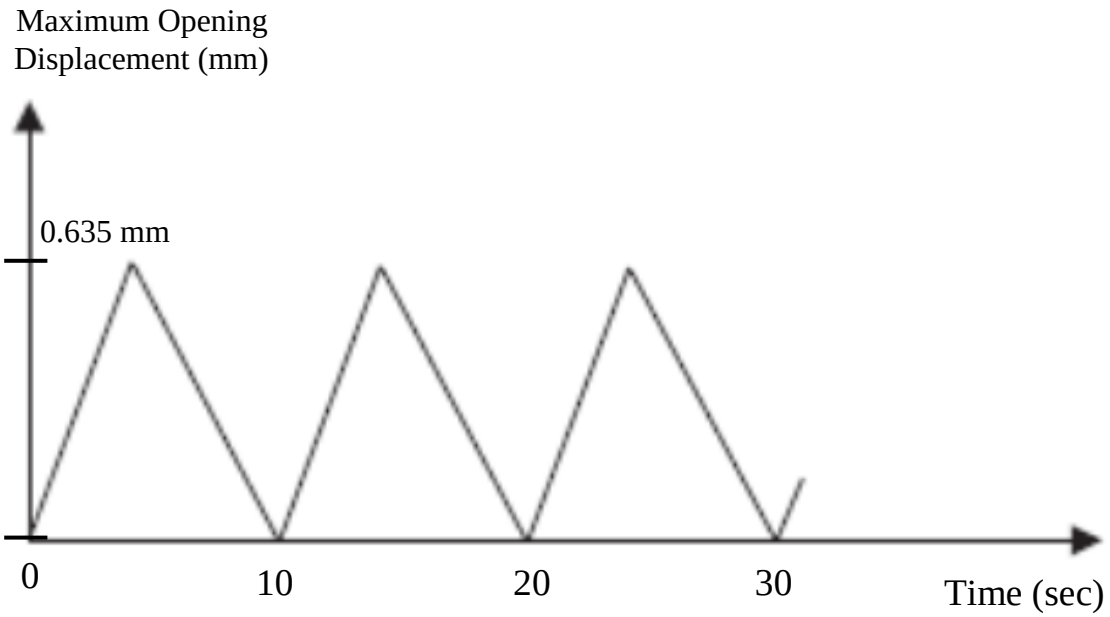

Figure 4. Overlay Tester load form (After Zhou, et al., 2007).

There is no universally accepted criteria for N_f for all pavement applications. Initially, Zhou and Scullion (2005) recommended that the pass/fail criterion be >300 N_f for reflective cracking and >750 N_f for reflective cracking with the presence of a rich bottom layer. The >300 N_f criterion was intended to be only applied to reflective cracking but the value worked well for predicting fatigue cracking as well (Zhou, et al., 2007). The OT is also used in New Jersey as 45% of the NJDOT roads are asphalt overlays on portland cement concrete (Bennert & Maher, 2008). In 2013, NJDOT recommended >150 N_f for surface mixtures with high RAP and PG 64-22 binder and >175 N_f for surface mixtures with high RAP and PG 76-22 binder (Sheehy, 2013). Bennert (2009) has used the OT extensively as a mix design and screening test to design better overlays in New Jersey (Bennert, 2009). A modified OT with further analysis required has also been used to estimate fracture energy and fracture resistance parameters (Zhou, et al., 2009).

2.4 NCAT Modified Overlay Test

The NCAT modified Overlay Test (NCAT-OT) was developed in 2014 (Ma, 2014). The test preparation and setup are exactly the same as described in Tex-248-F with two exceptions: 1) testing frequency and 2) maximum opening displacement. The NCAT-OT is performed at 1 Hz instead of 0.1 Hz because during his study, Ma (2014) found that at certain maximum opening displacement levels the resulting N_f values at 0.1 Hz were very similar to the 1 Hz results. Therefore, the faster frequency was proposed to reduce testing time. Also, the NCAT-OT uses a much smaller maximum opening displacement value than 0.635 mm required in Tex-248-F. Originally, researchers at the Texas Transportation Institute chose 0.635 mm to simulate the expansion and contraction of portland cement concrete joints in Texas. However, Tran, et al. (2012) and Ma (2014) proposed smaller maximum opening displacements values to better simulate conditions in flexible pavements. Smaller displacement values were selected because asphalt pavements would not expand and contract as much as portland cement concrete. Three different MODs were analyzed and 0.381 mm resulted in a combination of the most repeatable results and shortest testing time. Therefore, a maximum opening displacement of 0.381 mm was selected for the NCAT-OT method.

The final difference between the TX-OT method and the NCAT-OT method is the failure definition. Following the concept proposed by Rowe and Bouldin (2000) for the bending beam fatigue test, Ma (2014) used the peak of the "normalized load x cycle" curve to identify the transition from micro-crack formation to macro-crack formation and thus, failure. A comparison between the failure definitions of the two OT methods is shown in Figure 5. The cycle that corresponds to the maximum product of the load and the cycle is reported as the N_f for the test.

Ma (2014) reported significantly lower CV values for this method when compared to the Tex-248-F method. Furthermore, the normalized load x cycle failure definition more closely matched the point at which cracks propagated completely through the specimen as evident in video analysis.

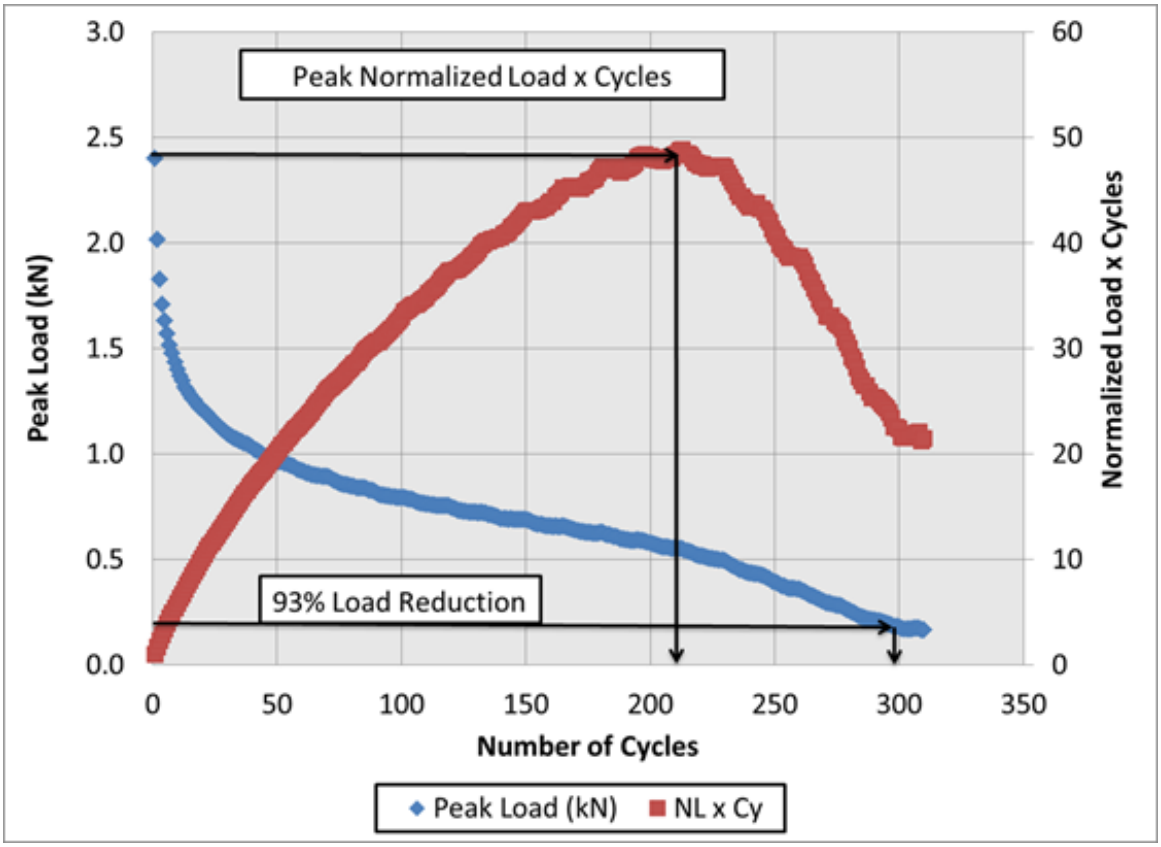

Figure 5. Determination of failure point for NCAT-OT vs. TX-OT.

2.5 Semi-circular Bend Test

The semi-circular bend test (SCB), although originally used to characterize fracture mechanisms of rocks (Chong & Kuruppu, 1988), has been used by researchers to measure several different properties of asphalt mixtures for over a decade. In the asphalt research community, variations of the SCB test have been used to assess low-temperature fracture resistance, estimate tensile

strength, and determine fatigue resistance (Li and Marasteanu 2004; Molenaar, et al., 2002; Arabani and Ferdowsi, 2009; Huang, et al., 2009; Kim, et al., 2012). Each of these studies used a different specimen geometry to determine the desired asphalt mixture property. Cracking potential has been shown to be best estimated by using notched specimens and calculating the critical strain energy release rate, or the J-integral (Jc). The Jc concept was first introduced to asphalt mixtures by Mull, et al. (2002) to determine fracture characterization of mixtures with crumb rubber in 2002. Since then, the J-integral has been used extensively in Louisiana to determine fatigue resistance in asphalt mixtures (Kim, et al., 2012). They investigated the fracture resistance of asphalt mixtures using SCB and IDT test results and found a good correlation with the IDT Toughness Index for lab produced mixtures even though the SCB results had absolutely no correlation with IDT strength results. They also determined that the Jc correlated well with field cracking data despite an average CV of 20% from 86 test mixtures. Wu, et al. (2005) analyzed the sensitivity of Jc to a wide variety of mixture variables and found significant effects from changing NMAS, binder type, and N_{design}.

The Louisiana DOTD recommends the SCB test for fracture characterization using asphalt specimens with three different notch depths of 25.4, 31.8, and 38.1 mm (Cooper III, et al., 2016). SCB specimens are loaded in a three-point bending test at a rate of 0.5 mm/min, measured by an LVDT. Strain energy to failure, U, is recorded from the test results by measuring the area under the load-displacement curve to the peak load, as shown in Figure 6. Figure 7 demonstrates how the strain energy values are then plotted against notch depth for each of the specimen replicates to create a negative linear trend line where the slope, dU/da, is used to calculate the Jc value, as shown in Equation 3. Larger Jc values indicate higher fracture resistance. Louisiana uses 0.45 kJ/m^2 as the minimum pass/fail threshold for asphalt mixtures (Cooper III, et al., 2016).

$$J_C = -\left(\frac{1}{b}\right)\frac{dU}{da} \quad [3]$$

Where:

Jc	=	Critical strain energy release rate (kJ/m^2)
b	=	Sample thickness (mm)
a	=	Notch depth (mm)
U	=	Strain energy to failure (N-mm)
dU/da	=	Change of strain energy with notch depth

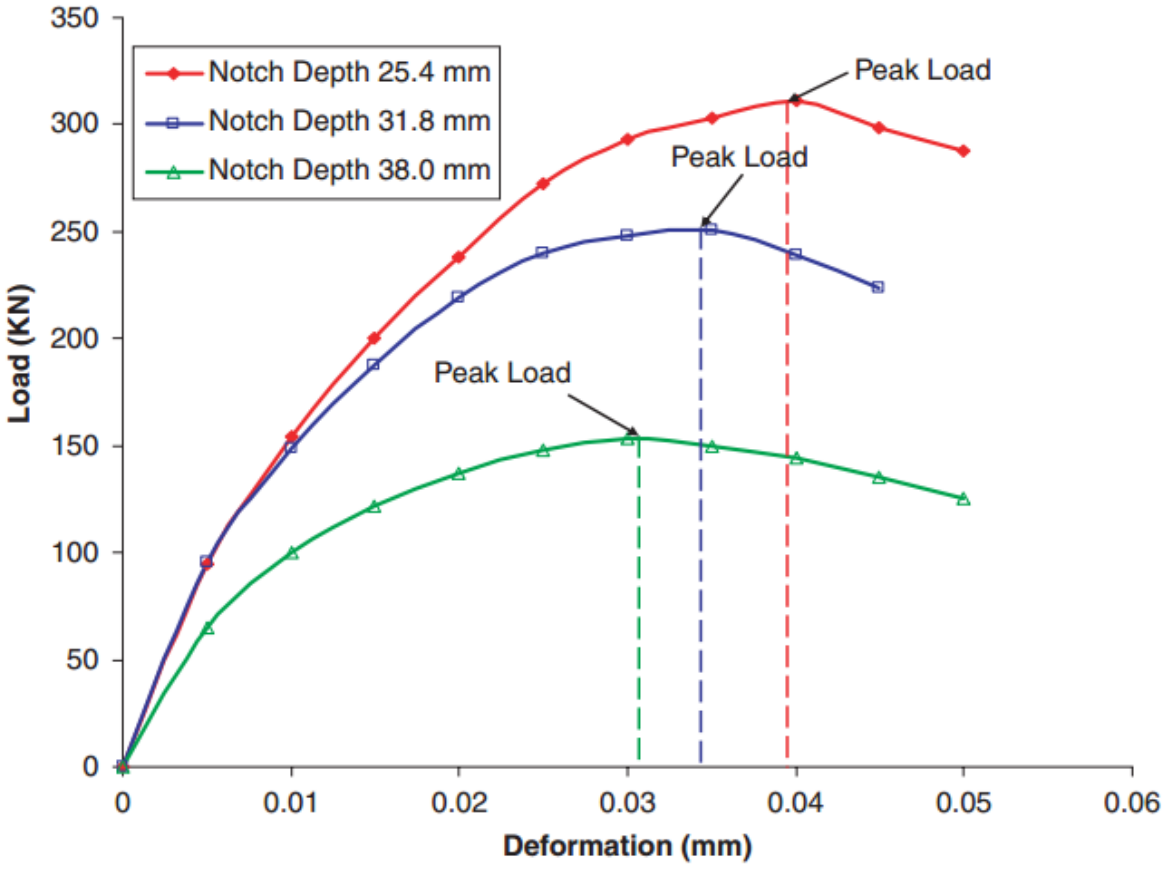

Figure 6. Load vs. displacement of typical SCB (Cooper III, et al., 2016).

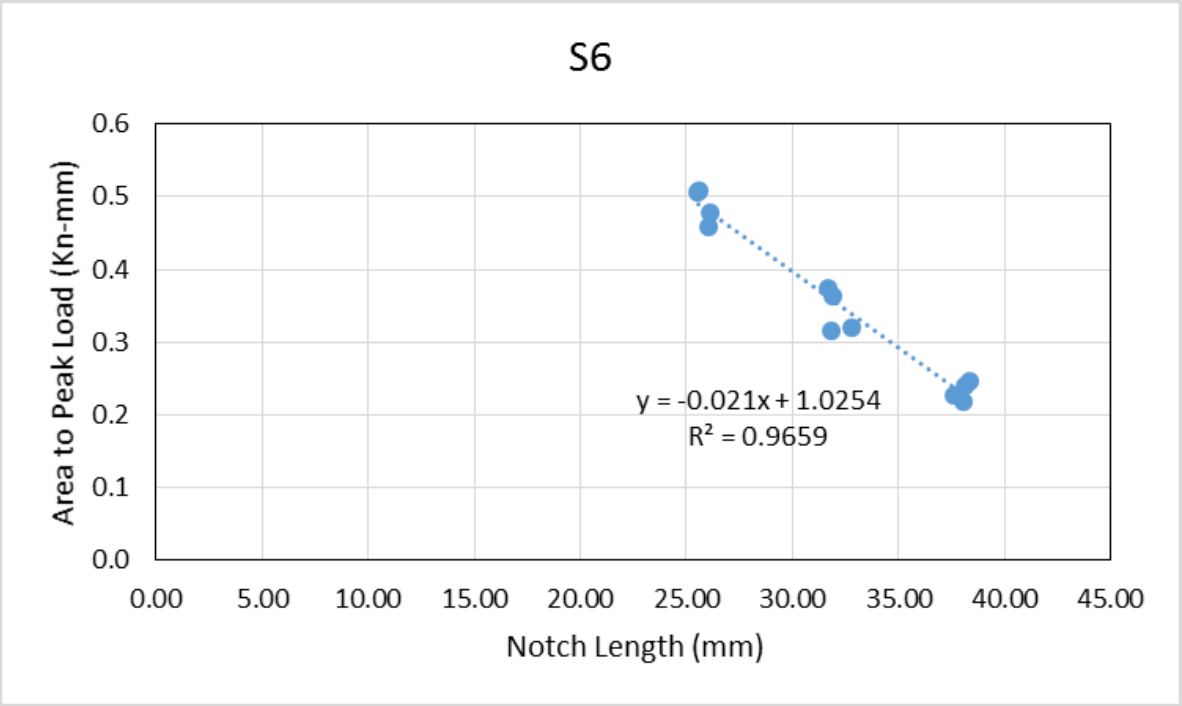

Figure 7. Area under load-displacement curve vs. notch depth.

2.6 Illinois Flexibility Index Test

Researchers at the University of Illinois developed a cracking test to screen out potentially poor performing mixtures with high amounts of RAP and RAS. The Illinois Flexibility Index Test (IFIT) was developed to address the lack of a cracking test that provided good field correlation, had a significant spread of test results, was repeatable and practical, and correlated to other current cracking tests (Ozer, et al., 2016a). The IFIT uses a fracture energy approach to determine cracking resistance in semi-circular asphalt specimens but the researchers recognized that fracture energy alone could not accurately distinguish between good and poor performing mixtures (Ozer, et al., 2016b). Fracture energy results from low temperature testing were unable to separate mixtures regardless of very different mixture and specimen properties like compaction level, binder types, ABR, and aggregate (Ozer, et al., 2016a). Testing at 25°C and a

loading rate of 50 mm/min produced results with a wide and distinguishable spread of fracture energy at a significance level of 0.10. An index parameter was added to the test procedure to improve reliability and prediction accuracy (Ozer, et al., 2016a). The Flexibility Index (FI) is calculated in Equation 4:

$$FI = A \times \frac{G_f}{|m|} \quad [4]$$

Where:

FI	=	Flexibility Index
G_f	=	Fracture Energy (J/m^2)
m	=	Inflection point of the post-peak load vs. displacement curve
A	=	Scaling factor (0.01)

Figure 8 shows a typical output of IFIT testing. The slope of the post-peak portion of the curve, m, was found to be highly indicative of mixture performance when given changes in testing conditions and material properties (Ozer, et al., 2016a). Steep slopes are the result of more brittle mixtures while more gradual slopes are produced by mixtures that exhibit the ability to slow crack growth after crack initiation. Currently, the Illinois DOT (2015) uses a FI of 8 as the preliminary minimum criterion for asphalt mixtures but more work is required to further calibrate the test to different traffic levels, climates, and mixture types and applications (Ozer, et al., 2016b). Typical CV values range between 10-20% (Al-Qadi, et al., 2015).

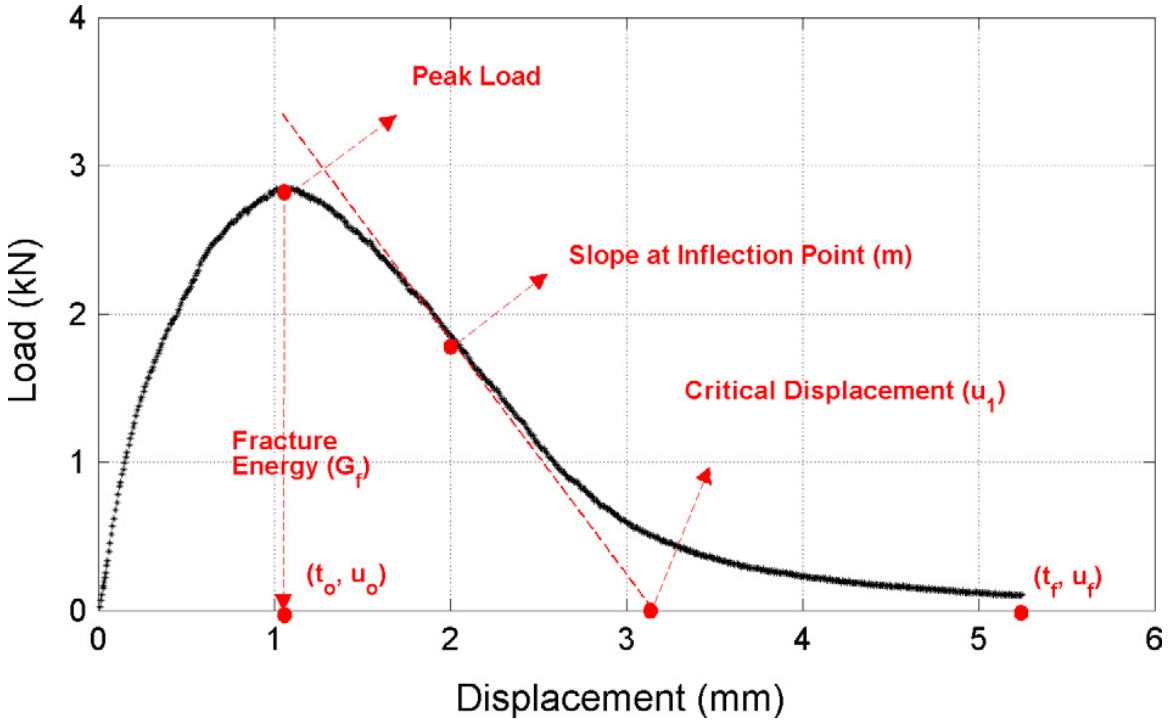

Figure 8. Typical result of IFIT test (Ozer, et al., 2016a).

2.7 Summary of Cracking Tests

Table 2 includes a summary of the load type, temperature, result, and typical variability of the five cracking tests. The following section summarizes these test methods and data analysis processes.

Table 2. Summary of properties of cracking tests in experiment.

Cracking Test	Loading Type	Temperature	Result	Typical Variability
Energy Ratio	Cyclic haversine waveform (Resilient Modulus) Monotonic vertical axis loading (IDT) Static loading (Creep Compliance)	10 °C	ER (ratio of $DCSE_{HMA}$ to $DCSE_{MIN}$)	N/A
Texas Overlay Test	Displacement-controlled cyclic loading to 0.635 mm.	25 °C	N_f (number of cycles to 93% load reduction)	30-50% CV
NCAT Overlay Test	Displacement-controlled cyclic loading to 0.381 mm.	25 °C	N_f (number of cycles to peak of normalized load x cycle curve)	20-30% CV (limited number of studies)
SCB	Monotonic three-point bending at 0.5 mm/min.	25 °C	J_c (Critical J-Integral)	20% CV
IFIT	Monotonic three-point bending at 50 mm/min.	25 °C	FI (Flexibility Index)	10-20 % CV (limited number of studies)

CHAPTER 3 – METHODOLOGY

This section summarizes the acquisition and properties of the asphalt mixtures, the methodologies followed to perform the five cracking tests, and the statistical analyses used to summarize the performance data. Brief descriptions of design and construction of the test mixtures are also included in this section.

3.1 Test Mixtures

3.1.1 Mixtures used in Experiment

Seven asphalt mixtures were selected by the experiment sponsors and were including in this study. Each mixture was placed as a surface lift on the NCAT Test Track on top of rich, highly polymer-modified base and binder layers, as shown in Figure 9. The target thickness of the surface lifts was 1.5 inches. Only the surface course mixtures of the sections were analyzed in this study. The base and binder courses were designed to be highly elastic to reduce the probability of bottom-up fatigue cracking and isolate top-down cracking as the primary mode of pavement distress. Table 3 includes a summary of the in-place properties of the seven mixtures. The mixtures were designed to cover a wide range of cracking susceptibility to evaluate both the cracking tests discussed later and the effect of various mixture properties on top-down cracking. More details regarding the specific properties of each test section are included in Appendix A.

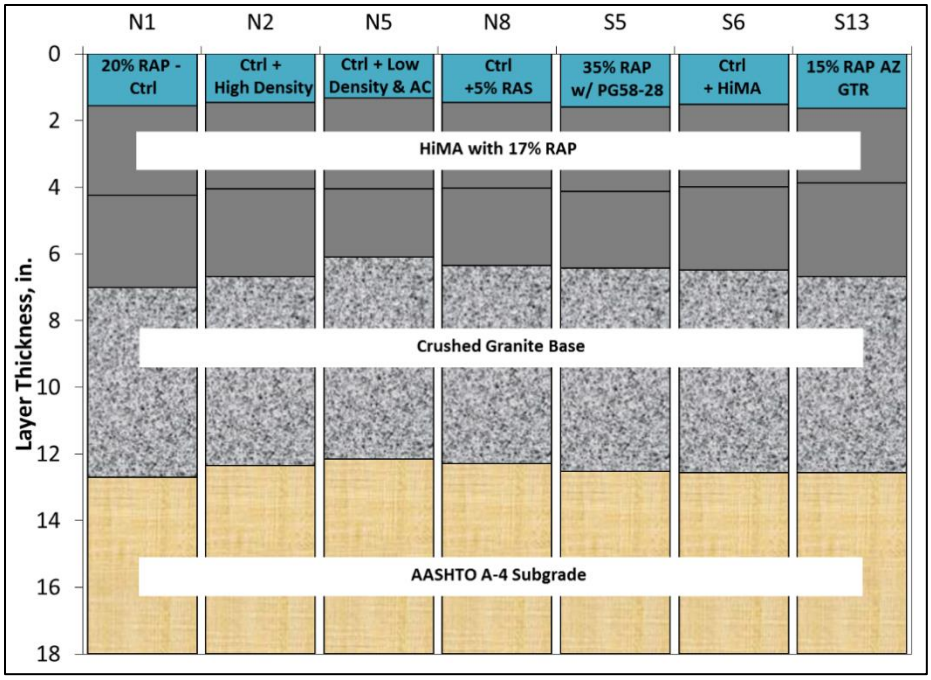

Figure 9: Cross sections of experimental test sections.

3.1.1.1 N1 – 20% RAP – Control Mixture

The mixture designated as the control in this experiment was designed with 20% RAP and PG 67-22 binder. This mixture is not a true "control" although some of the other mixtures were slight deviations from this mixture. This mixture was the most basic in the experiment and was expected to have moderate cracking susceptibility. The resultant effective binder grade of the mixture was PG 88-16 because of the 17.7% asphalt binder ratio (ABR) from the RAP. This mixture was designed as a typical 20% RAP mixture and was expected to exhibit medium cracking susceptibility.

Table 3. TDC Experiment mixtures.

Mixture	NMAS (mm)	Avg. Thickness (in)	In-place %G_{mm}	Target V_a (%)	QC VMA (%)	QC P_{be} (%)	Recycled Asphalt Binder Ratio	Extracted Binder Grade	Expected Cracking Susceptibility
N1 - 20% RAP (Control)	9.5	1.6	93.6	7.0	14.7	4.7	0.177	88.6 – 16.6	Medium
N2 - Ctrl + High Density	9.5	1.5	96.1	4.0	14.7	4.7	0.179	88.9 – 15.9	Low
N5 - Ctrl + Low Density & AC	9.5	1.3	90.3	10.0	15.4	4.4	0.189	88.0 – 18.5	High
N8 - Ctrl + 5% RAS	9.5	1.5	91.5	7.0	14.4	4.8	0.372	107.3 – 5.4	High
S5 - 35% RAP w/ PG 58-28	9.5	1.6	92.2	7.0	15.1	5.1	0.292	82.8 – 23.0	Medium
S6 - Ctrl w/ HiMA	9.5	1.5	91.8	7.0	14.7	5.0	0.166	101.4 – 21.5	Low
S13 - 15% RAP AZ GTR	12.5	1.6	92.7	7.0	18.4	6.6	7.5	N/A	Low

3.1.1.2 N2 – 20% RAP (Control) + High Density

The high density mixture was the same mix design as the control mixture except that it was compacted to 96.1% Gmm in the field. This mixture was expected to perform very well in terms of cracking resistance due to the extra density in this section.

3.1.1.3 N5 – 20% RAP (Control) w/ Low AC & Low Density

The low density mixture used the same aggregate mix design as the control section but had a target asphalt content of 0.7% less than the control mixture. This section resulted in an average in-place density of 90.3% Gmm after construction. Due to the low asphalt content and high air voids, this section was expected to perform poorly in terms of top-down cracking resistance.

3.1.1.4 N8 – 20% RAP (Control) + 5% RAS

The RAS mixture had a similar aggregate structure to the control mixture with minor changes in the proportions of 89 granite aggregate and sand being incorporated to allow for RAS in the mixture. It was expected that the ABR from the RAS and RAP would exceed 35% so the amount of virgin binder used was only 5.0%. The QC samples confirmed the ABR expectation as the ABR was 37.2%. The extra stiffness from the recycled materials caused this section to be extremely difficult to compact to target density. Special heating equipment used for hot-in-place recycling (Figure 10) was brought in to heat the surface lift of this section after the contractor had already compacted it as much as possible. The surface was heated to the compaction temperature with the heating equipment and then immediately compacted with rubber tire rollers. This process took several hours and resulted in a final density of 91.5% Gmm. Due to the extreme stiffness of this mixture and the low in-place density, this mixture was expected to be one of the poorest performing sections in this experiment.

Figure 10: Hot-in-place recycling equipment on Section N8.

3.1.1.5 S5 – 35% RAP w/ PG 58-28

The section with increased RAP percentage and a lower binder grade was designed with 9% less granite 89s, 5% less granite M10s, and 1% more sand than the control section. The materials were the same but the proportions were changed to allow for the extra 15% RAP. S5 was constructed with a lower grade of binder in accordance with typical binder grade bumping practice when high RAP contents are used. The PG 58-28 binder was modified with SBS. The balanced combination of high ABR with a lower grade of asphalt was expected to produce a medium performing mixture.

3.1.1.6 S6 – 20% RAP (Control) w/ HiMA

This section was the same aggregate structure as the control mixture but used highly polymer-modified asphalt (HiMA) as binder instead of PG 67-22. The binder used to construct the surface

lift of S6 was the same binder used to construct the rich base and binder courses of all seven mixtures in the experiment. Due to the high elasticity of the HiMA binder, this section was expected to have high resistance to TDC.

3.1.1.7 15% RAP w/ AZ GTR

Mixture S13 was constructed as a gap-graded, 12.5 mm mixture with ARB20 (PG 67-22 with 20% GTR) binder. The different gradation, NMAS, binder type, and high binder content made this mixture very different than the other six mixtures. The rubber modified binder was expected to yield very high TDC resistance.

3.1.2 Mixture Sampling

Asphalt mixture samples for this study were collected during the construction of the 2015 NCAT Test Track in Opelika, Alabama. A material transfer device unloaded a large amount of mix onto a flatbed truck where the mix was later shoveled into 5-gallon buckets. The buckets were reheated to the compaction temperature of the mixtures and test specimens were fabricated using a Superpave Gyratory Compactor (SGC). Therefore, the results reported in this thesis are only for reheated plant mixed-lab compacted (PMLC) specimens. Further studies will be conducted to investigate lab-mixed and lab-compacted specimens as well as long-term aged specimens but are outside the scope of this thesis.

3.2 Energy Ratio

The Energy Ratio (ER) was determined by combining the results of three test procedures: resilient modulus, creep compliance, and indirect tensile strength. All of these tests were performed at 10°C with an MTS® servo-hydraulic testing device. Four specimens were

compacted using with a Superpave Gyratory Compactor (SGC) to a height of 125 mm and a diameter of 150 mm trimmed to a thickness of 38-50 mm using a saw. The target post-cut air voids were within 0.5% of the target air voids for each mix listed in Table 3. Extensometers were attached to each face of the specimen to measure vertical and horizontal deformations of both faces separately, as shown in Figure 11. Results from each test were recorded for each side of the specimen and used to obtain a trimmed mean with the highest and lowest values being discarded.

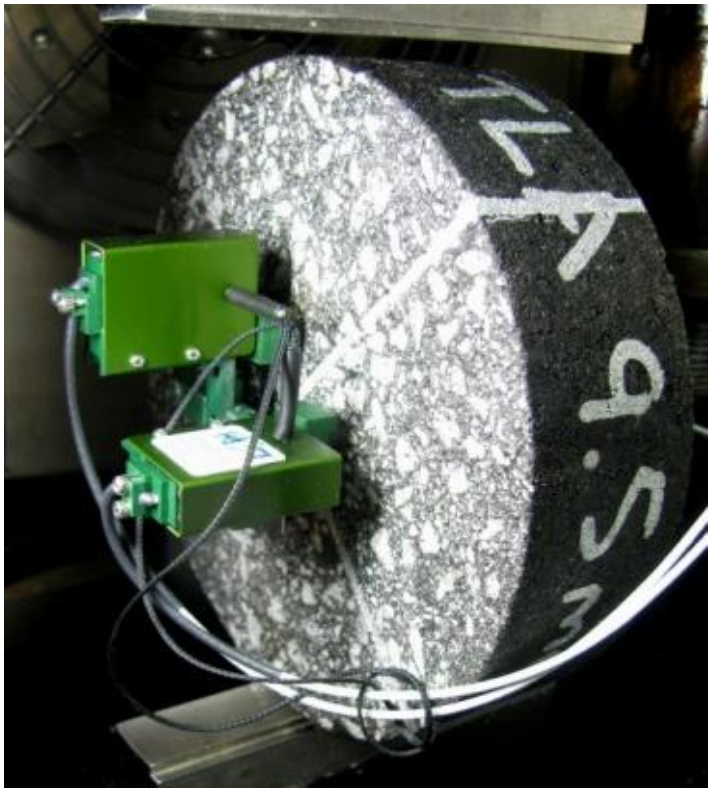

Figure 11: Energy Ratio specimen with vertical and horizontal extensometers.

The resilient modulus was determined using a haversine waveform load during load-controlled testing mode. ASTM D7369-11 specifies that an indirect tensile strength test should be run before performing the resilient modulus test. However, since four samples were created but only three were tested, the extra sample was used as a dummy sample to guess the initial loads required for the non-destructive tests in the ER. Experience shows that an initial load of about

2000 lbs. yields a horizontal strain within a target range of 100-200 με. The large load was required due to the reduced testing temperature. The reduced temperature also eliminated the required 100 preconditioning test cycles due to the extremely reduced specimen deformation at the low temperature. One load cycle consists of a 0.1 second load pulse and a 0.9 second rest period. Horizontal and vertical deformations were recorded for five cycles and used to determine the resilient modulus. All data collection and processing were performed in the Energy Ratio software from the University of Florida (Roque, et al., 1997).

Creep compliance was determined immediately after the resilient modulus. Since both tests were non-destructive, they were performed in succession before the indirect tension test. The same dummy sample used to guess the initial load for the resilient modulus was used to guess the static load for the creep compliance test. Experience shows that an initial load of about 250 lbs. for 1000 seconds suffices to produce horizontal deformations between 0.00125 and 0.0190 mm. The horizontal and vertical deformations were recorded for each face for three specimens and a trimmed mean deformation was determined by discarding the highest and lowest deformations. The remaining deformation values were used to determine the creep compliance. Creep compliance power function properties (m, D_0, and D_1) were determined by curve-fitting the test results. All data collection and processing were performed in the Energy Ratio software from the University of Florida (Roque, et al., 1997).

Finally, the indirect tensile strength was determined by applied a load at a constant rate of 12.5 mm/min until the peak load was reached. The peak load was used to calculate the IDT strength (S_t) and the DCSE was calculated by integration of the resulting stress-strain curve. The results from the three tests were analyzed in the provided software. Trimmed means of each of the

values were determined and used to calculate the Energy Ratio value using the previously shown equations.

3.3 Texas Overlay Test

All TX-OT testing was performed on an Asphalt Mixture Performance Tester (AMPT) (IPC Global, 2012) and in accordance with Tex-248-F. TX-OT specimens were compacted in a SGC to a target height of 125 mm. Tex-248-F requires that one specimen per gyratory pill be used for testing; however, a sensitivity analysis performed by Walubita et al. (2012) recommended using two specimens per gyratory pill to improve efficiency. Therefore, two specimens per pill were cut to 150 mm long by 75 mm wide by 38 mm thick, as shown in Figure 12a. The air voids for the cut specimens were selected as the target in-place air void content ± 1.0 percent. The specimens were glued to two steel plates using a two-part epoxy and a ten pound weight, shown in Figure 12b and Figure 12c, respectively. A 4.2 mm piece of tape, shown in Figure 12d, was placed along the surface of the specimen between the two plates where the crack would initiate to prevent any epoxy from contaminating the specimen surface.

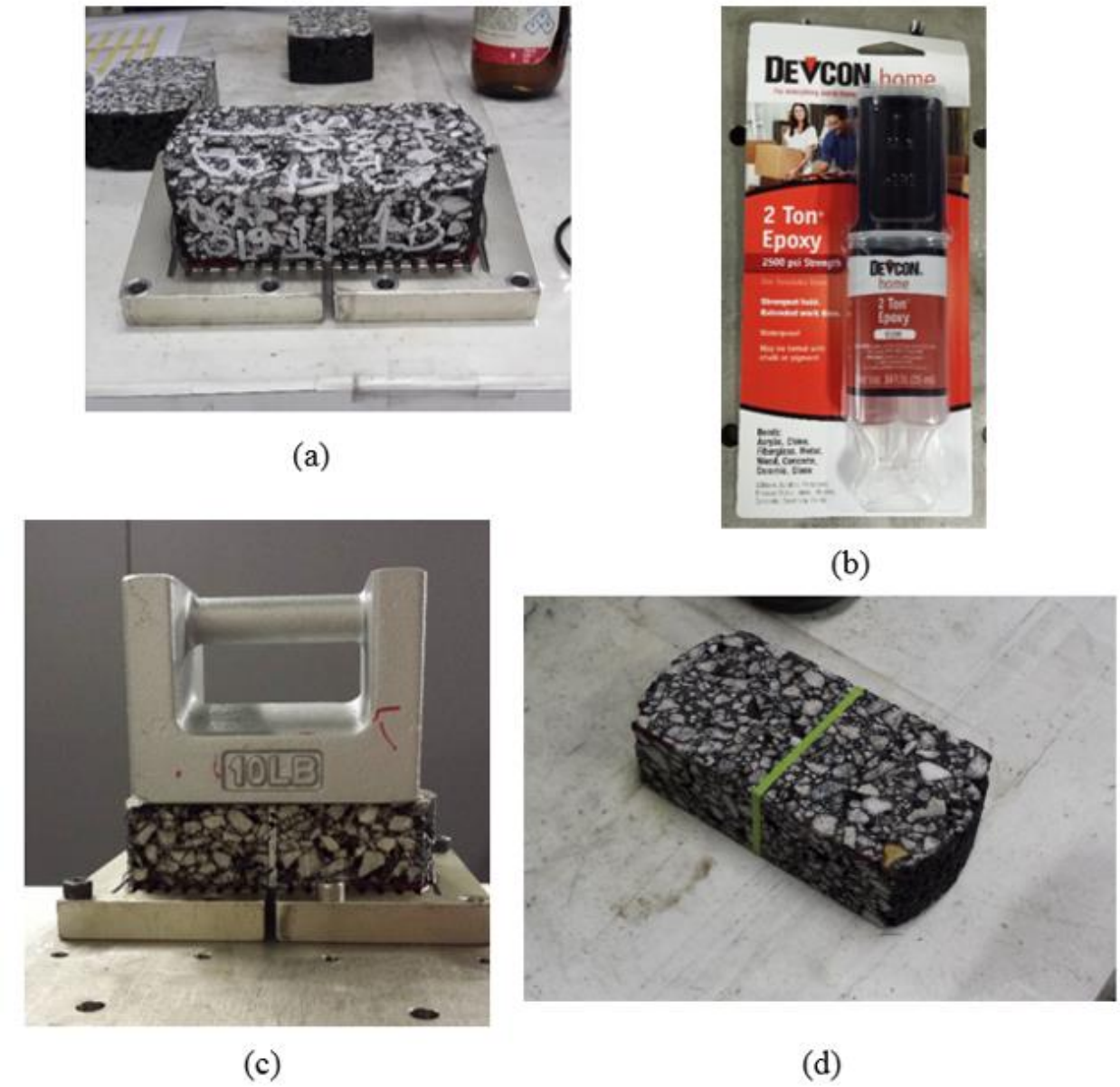

Figure 12: (A) Overlay specimen glued to two plates. (B) Epoxy used for OT testing. (C) Gluing OT specimen to plates. (D) Tape used to prevent epoxy from contaminating crack surface.

Four specimens per mixture were tested at 25°C in displacement controlled mode. Loading was applied by moving one of the steel plates away from a fixed plate at a rate of one cycle every 10 seconds. Each cycle consisted of a five second loading phase and a five second unloading phase

with a sawtooth waveform and maximum opening displacement per cycle of 0.635 mm. The maximum load applied during each cycle was recorded. The test continued until the applied loads decreased by 93% from the initial cycle and the cycle that produced the 93% load reduction load was recorded as the N_f.

3.4 NCAT Modified Overlay Test

The NCAT modified OT (NCAT-OT) uses the exact same sample preparation as the Texas method explained previously. The only differences between the two testing methods are 1) loading frequency, 2) maximum opening displacement, and 3) method of defining cycles to failure. The NCAT-OT test is conducted at a frequency of 1 Hz and uses a maximum displacement of 0.381 mm. After testing, the load recorded for each cycle is multiplied by total number of cycles to create a normalized load. The failure definition of NCAT-OT specimens is the peak of the "normalized load x cycle" (NLC) curve. Figure 13 demonstrates a typical output from the NCAT-OT and the failure definition.

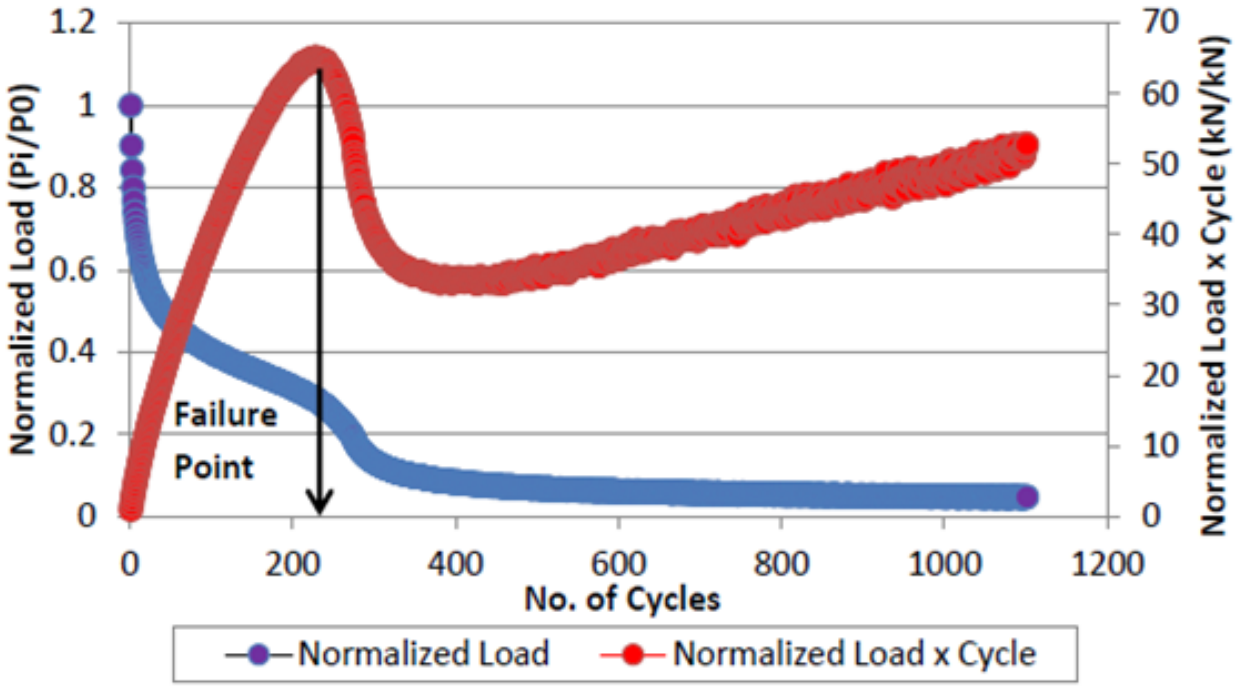

Figure 13. Failure definition of NCAT-OT method (Ma, 2014).

3.5 Semi-circular Bend Test

SCB testing was performed in accordance with a draft specification from the Louisiana Transportation Research Center (LTRC). SGC specimens were compacted to a height of 57 mm and cut in half to produce semi-circular specimens. Twelve SCB specimens with air voids within 0.5 percent of the target air void content of each mixture were needed for a complete SCB analysis. The notches were cut using a saw and a mold fabricated to secure the SCB specimen during the notch cutting process. Figure 14 shows the mold and Figure 15 shows the saw used to cut the notches.

Figure 14: SCB/IFIT trimming mold

Figure 15: SCB/IFIT trimming saw

The notches were cut to depths of either 25.4, 31.8, or 38.1 mm, shown in Figure 16. Four specimens at each notch depth are necessary for SCB analysis. The notch width for all specimens was 3 ± 0.5 mm.

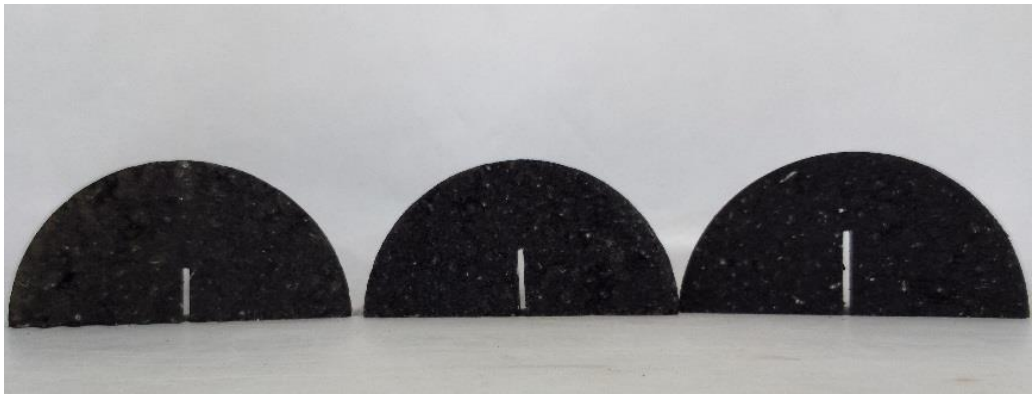

Figure 16. SCB-LTRC notched specimens.

These specimens were temperature conditioned in an environmental chamber at 25 ± 0.5°C for two hours prior to being tested. The specimens were loaded monotonically using an AMPT in a three-point bending device at a rate of 0.5 mm/minute using the setup shown in Figure 17. From each specimen, a plot of load versus displacement (measured with an external LVDT) was collected. For each data file, numerical integration was used to determine the area under the load-displacement curve to the peak load. Finally, a regression was performed for these area values against their corresponding specimen notch depths. The slope of the regression lines was used to determine the critical J-Integral (J_c) value for each mix.

Figure 17. SCB-LTRC test setup using an AMPT.

3.6 Illinois Flexibility Index Test

IFIT testing was performed in accordance with a draft specification from the Illinois Department of Transportation using a standalone IFIT testing device. SGC specimens were compacted to 160 mm and trimmed to obtain four semi-circular specimens from the gyratory specimen. IFIT specimens were fabricated using the same saw and mold used for SCB testing but with a thinner blade and a shorter notch depth. A 15 ± 1 mm deep and 1.5 mm wide notch was cut in the center of the base of the semi-circular specimen, as shown in Figure 18. Prior to testing, specimens

were placed in an environmental chamber at 25 ± 0.5 °C for 2 hours. Testing was performed using the device shown in Figure 18.

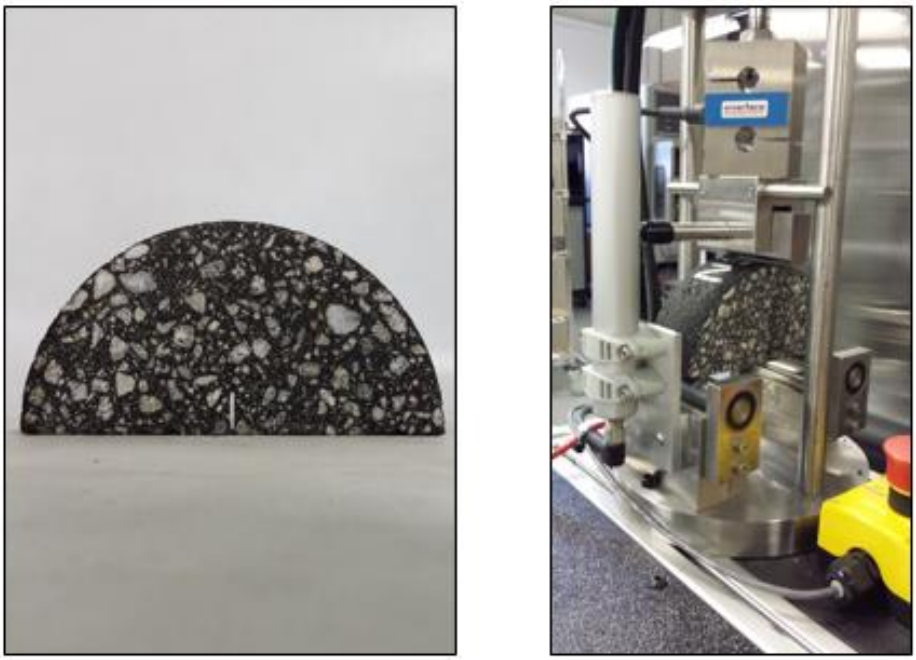

Figure 18: IFIT Notched Specimen and Test Setup

The load was applied monotonically at a rate of 50 mm/min until the measured load decreased to less than 0.1 kN. Force and displacement data were collected at a rate of 50 Hz by the test system and computer. All data analyses are performed using the software provided with the IFIT testing device and developed by the Illinois Center for Transportation (ICT) at the University of Illinois at Urbana-Champaign (UIUC). Fracture energy and the post-peak slope of the inflection point of the load vs. displacement curve were determined and used to calculate the Flexibility Index.

3.7 Statistical Analyses

The statistical analyses methods used for this study were intended to determine if results for each test were significantly different among the seven mixtures. In the case of S13 (15% RAP AZ

GTR) and N8 (Ctrl +5% RAS), these two mixtures have very different binder contents and grades, aggregate gradations, volumetrics, and recycled binder replacement. Mixtures with such extreme differences in aggregate and binder properties were considered to have practical differences regardless of statistical results. The extremely small sample sizes and unequal variance between mixtures created limitations in the statistical testing for significant differences between two mixtures. Due to these limitations, performing an ANOVA and assigning mixtures to groups based on a valid statistical test were impossible. As the end goal of this study was to separate mixtures into groups based on results from the laboratory tests, mixtures were assigned tiers according to how the means and standard deviations compared with other means and standard deviations. For example, if Mixture A had a mean that was much larger than Mixture B and the standard deviations of the two mixtures did not create any overlap at one standard normal deviate away from the means, the mixtures were assigned to different tiers. Statistical testing was used to assess the validity of the assumed tiers. These laboratory result tiers will be compared with the tiers of the same mixtures in future work as well as with field performance. Statistical differences between mixtures were determined using two-sample t-tests for all OT and IFIT results, and linear regression was used for the SCB results. Statistical analyses of the data produced in this study were performed using Minitab ® version 16.2.2. The sample variances between mixture results for the IFIT and Overlay tests were not equal and the sample sizes were very small so comparing means using an ANOVA was invalid (Devore & Farnum, 2005).

All test results except the Energy Ratio were checked for outliers in accordance to ASTM E178-08 (ASTM International, 2008). This method utilized one-sample t-tests to compare each test result to a critical two-sided T statistic for each mixture. All results that yielded T scores more extreme than the critical T statistic at a significance level of 0.10 failed ASTM E178-08 and

were eliminated. A summary of basic statistics (replicates, average, standard deviation, and coefficient of variation) are provided for both OT methods and the IFIT method.

Energy Ratio results are a product of a pooled analysis of three laboratory tests. Each of the tests reported a value for both sides of the specimen. As three specimens were tested for each lab test, a total of six results were reported. The maximum and minimum values for each test were discarded and a trimmed mean was calculated based on the middle four results. The ER was then calculated as shown in Equations 1 and 2 using the trimmed mean results of the required variables. Therefore, although replicates are produced and tested in the ER process, statistical analyses of ER results were not possible because only one ER value was calculated for each mixture.

OT and IFIT results were analyzed and mixtures were assigned to tiers based on a comparison of the results, as discussed previously. The mixtures within each tier were compared to confirm whether or not the mixtures were statistically different. Special case two-sample t-tests assuming unequal variances among the mixtures were used to determine statistical differences between mixtures at a significance level of 0.05. If the resultant p-value of the t-test was less than the significance level, the null hypothesis that the mixtures were not different was rejected. This test required that both samples be independent and normally distributed. These requirements were assumed by the author as there was no historical evidence to indicate that the mixture results would not be normally distributed. If typical two-sample t-tests were used to determine differences between the means of seven mixtures, the probability of committing a Type I error, claiming that two mixtures were different when they were not, was 66%[1]. However, most of the

[1] 21 pairs at significance level of 0.05: $1-(0.95)^{21} = 66\%$

statistical differences between mixtures often involved either N8 (Ctrl + 5% RAS) or S13 (15% RAP AZ GTR). As discussed previously, these two mixtures exhibited practical differences between each other and many of the other mixtures. These two mixtures had the worst and best results for both the Overlay Test methods and the IFIT in terms of cycles to failure and Flexibility Index, respectively. In the case of the Overlay Tests, the cycles to failure (N_f) of S13 was a different order of magnitude from the other mixtures, and the N_f for N8 were the minimum possible value for the TX method and at least fifteen times lower than all other mixtures for the NCAT method. Therefore, it is assumed that most of the significant differences between the means of S13 and N8 and all other mixtures are true differences and not Type I errors.

Finally, SCB data were analyzed using linear regression by plotting strain energy (U) against notch depth (a) to determine the J-Integral (J_c) of each mixture. Since the J_c is essentially a generalization of the strain energy release rate for materials that exhibit elasto-plastic behavior (Wu, et al., 2005), and the strain energy release rate is used to assess crack tip propagation and not crack initiation (Hosford, 2005), the intercept value of the strain energy vs. notch depth curve is insignificant. The results of the SCB dU/da analyses were used to calculate the J_c for each mixture. The mixtures were then ranked using estimates of the mean and standard deviation of the slopes. The strain energy vs. notch depth relationship (dU/da) was the only variable used to calculate the J-integral (assuming that the specimen thickness was constant). The slope were multiplied by a constant, as shown in Equation 3, to determine the J_c for each mixture. The standard deviation of the dU/da slopes were multiplied by the same constant to scale the results to achieve the estimated standard deviation of each mixture's Jc value. It is important to note that there is no standard, or even commonly used, method to quantify and display J_c error, and that this method was developed by the author.

SCB data were analyzed in Microsoft Excel® to determine the mean slope for each mixture and the standard deviation of the slope. Strain energies at failure and the corresponding notch lengths were plotted for each mix and a best-fit line was calculated by Excel according to the least squares method. The built-in regression function in Excel were used to calculate the mean slope and the sum of squared residuals (SSResid) of the regression model. The mean square error (MSE) for the regression model was calculated as shown in Equation 5 and was required to obtain an estimate of the overall regression model deviance in both the x and y directions (Devore & Farnum, 2005).

$$\sigma_e^2 \approx s_e^2 = \frac{SSResid}{n-2} \qquad [\ 5\ ]$$

Where:

σ_e	=	Standard deviation of regression model population total error
s_e	=	Estimated standard deviation of regression model total error
SSResid	=	Sum of squared residuals
n	=	Sample size

Since the linear regression best fit line has two estimated parameters for slope (B) and intercept (α), both are affected by the total error of the model. The variability of the slope in the dU/da curve was required to determine the standard deviation of the Jc values and for the determination of the 95% confidence interval of the true mean of the dU/da slope. The standard deviation of the slope of the dU/da curve was determined using Equations 6 and 7 by assuming that the population variance and the sample variance within each mixture were equal, as shown in Equation 5. (Devore & Farnum, 2005).

$$s_b = \frac{s_e}{\sqrt{S_{xx}}} \quad [6]$$

Where:

s_b = Estimated standard deviation of the slope of the regression model

s_e = Estimated standard deviation of regression model total error

S_{xx} = Sum of squared differences between x-values (notch lengths)

and,

$$S_{xx} = \sum x_i^2 - \frac{(\sum x_i)^2}{n} \quad [7]$$

Where:

x_i = i^{th} value of x (notch length)

n = sample size

The standard deviations of the mixtures were used to visually demonstrate the variability of the Jc results of SCB testing. To allow for proper comparison between mixtures, the 95% confidence intervals of the dU/da slopes for each mixture were calculated using Equation 8 (Devore & Farnum, 2005).

$$CI = b \pm t^* \times s_b \quad [8]$$

Where:

CI = 95% confidence interval of regression slope

b = Slope of the least squares regression line

s_b = Estimated standard deviation of the slope of the regression model

Therefore, the 95% confidence intervals of the value of dU/da were determined and used to statistically compare mixture performance. If the confidence intervals of two mixtures did not overlap, the results of these mixtures were declared to be statistically different.

This chapter described the mixture design of each of the seven mixtures included in this study. It also included descriptions of each of the cracking tests utilized, the sample preparation required, and typical data analysis conducted. The results of the data analyses for each of the tests are presented in the next chapter.

CHAPTER 4 – RESULTS AND ANALYSIS

This section contains the results of the five cracking tests used in this experiment. The test results, variability, and statistical analysis of each test, except the ER, are included in this section. Also included in this chapter are discussions of the results of the mixtures in each test and a final average ranking of the seven mixtures over all five tests. The individual results of each test replicate are listed in Appendix B.

4.1 Energy Ratio

The results of the fracture energy, resilient modulus, $DCSE_{HMA}$, creep compliance, and energy ratio of the seven mixes are shown in Figure 19-Figure 23. Note that all mixtures except N8 with 20% RAP and 5% RAS had $DCSE_{HMA}$ values that exceeded the range of 0.75 – 2.5 kJ/m^3 listed in Table 1. The $DCSE_{HMA}$ for N8 was within the recommended range. It should be noted again that the ER parameters were calibrated using field cores of which most had been in place for at least 10 years (Roque, et al., 2004). The mixtures analyzed for this study were once-reheated plant mix. Had the mixtures been aged to simulate long-term field aging, the $DCSE_{HMA}$ results would have been lower. This fact is especially true for mixture N8. N8 met all the ER criteria and actually resulted in the highest ER by a large margin. However, this mixture is not expected to perform well in the field. The extremely high ER of N8 can be explained by the low creep rate of the mixture. Note that the creep rate for N8, shown in Figure 22, is at least four times lower than the other six mixtures. The ER calculation includes the creep compliance parameters in the denominator so low creep rates will yield high ER results. The opposite effect can be seen in mixture S13 with 15% RAP and GTR binder. S13 has the highest creep rate and not surprisingly, the lowest ER.

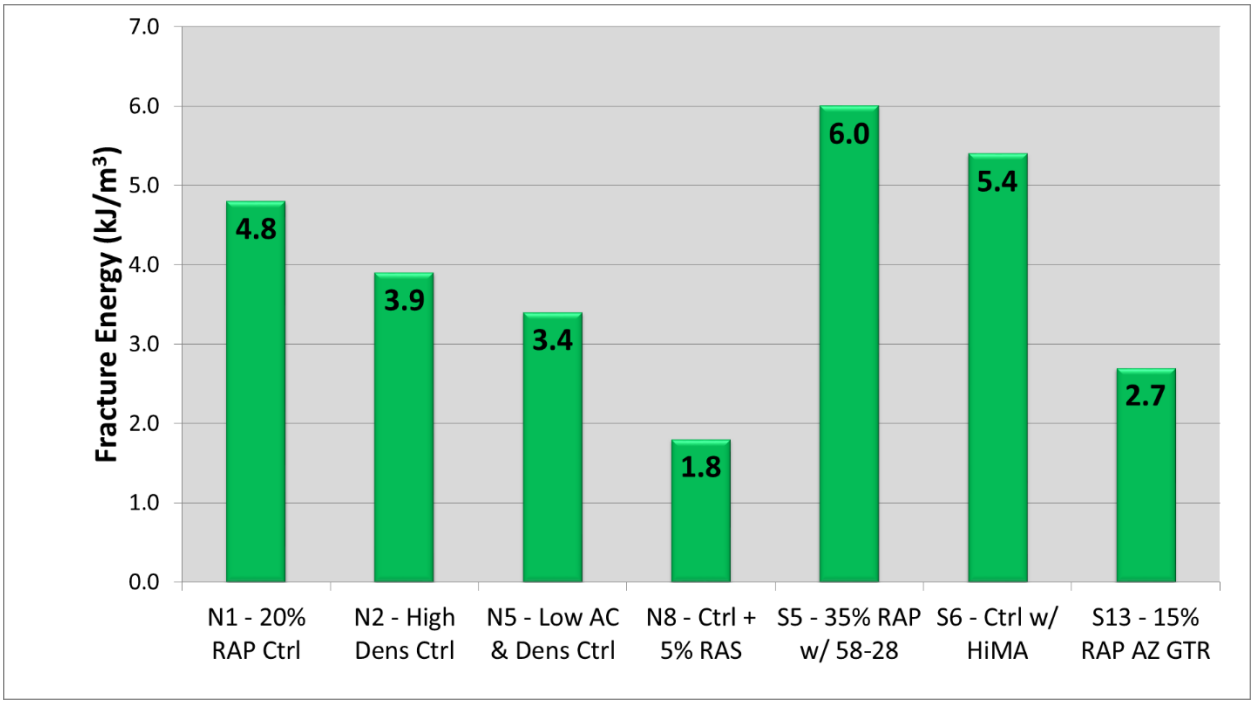

Figure 19: IDT Fracture Energy

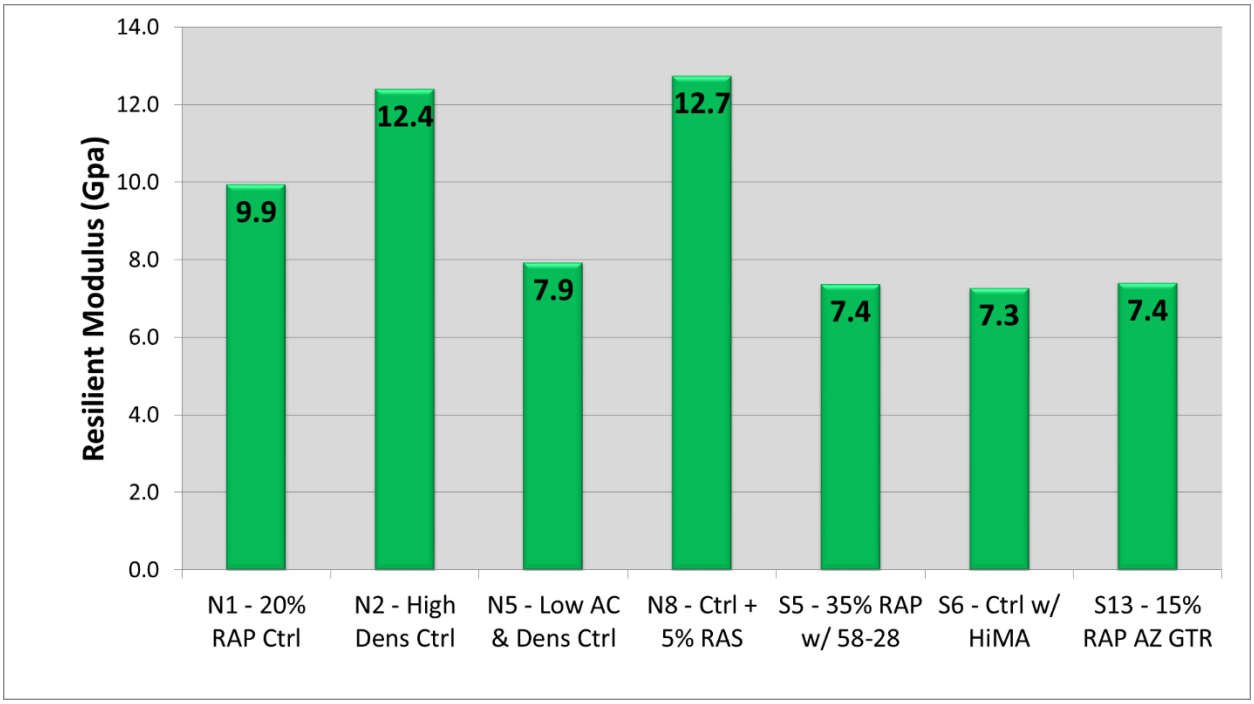

Figure 20: IDT Resilient Modulus

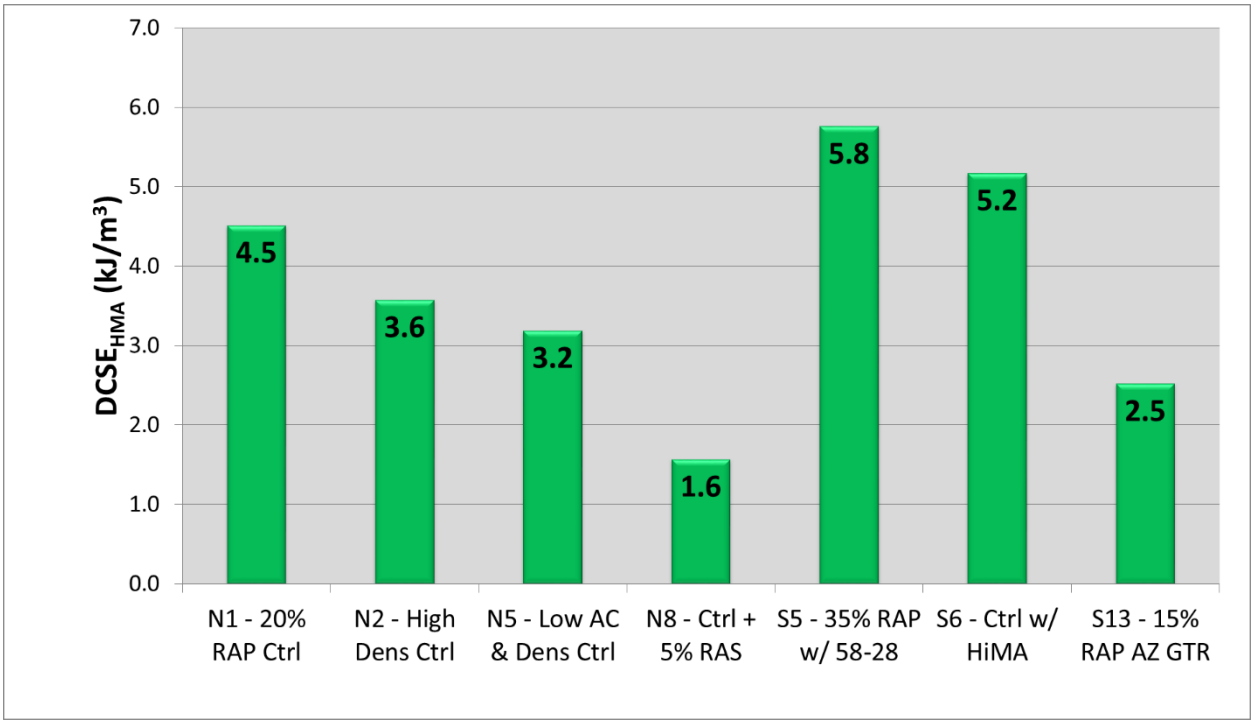

Figure 21: IDT DCSE$_{HMA}$

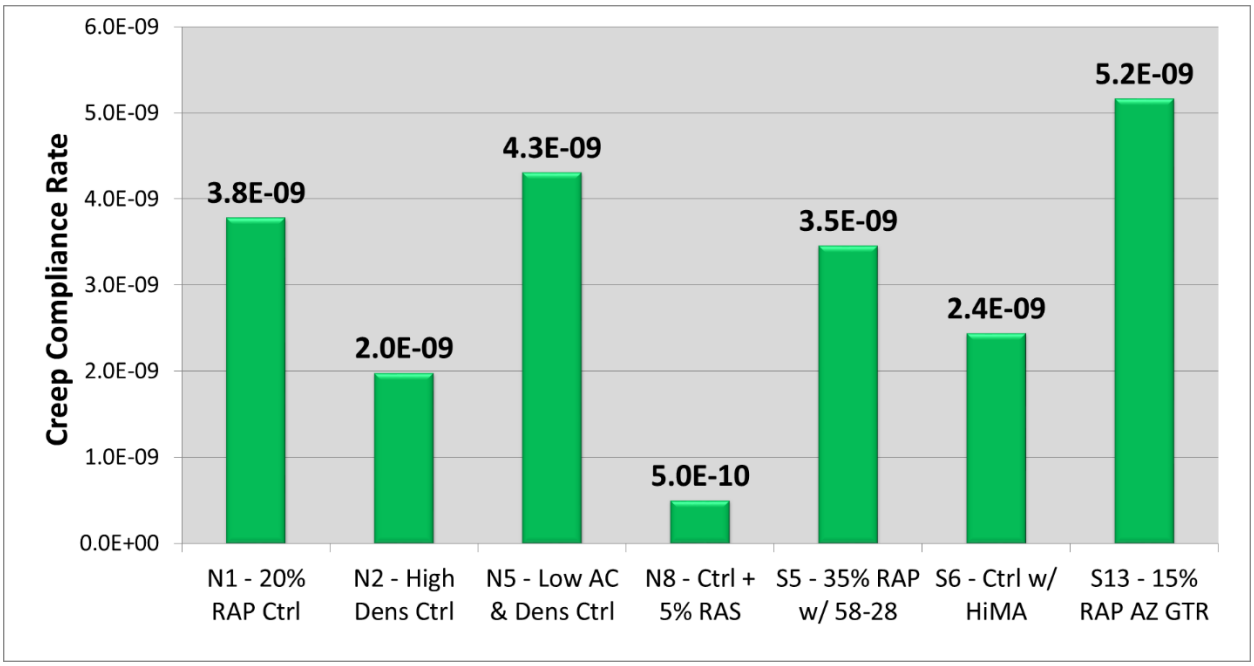

Figure 22: IDT Creep Compliance Rate.

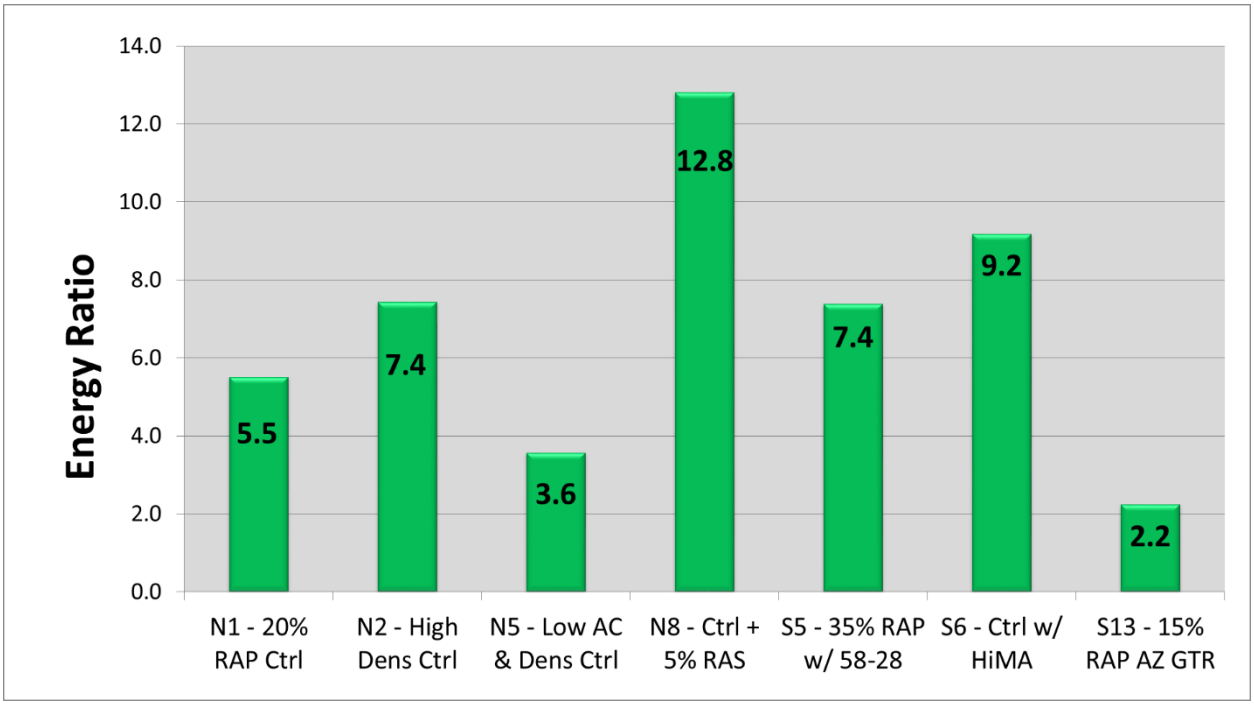

Figure 23: Energy Ratio Results

The ER results appear to distinguish between high and low density mixtures in N2 and N5, respectively. With the exception of S13 with GTR binder, the mixtures with soft or polymer-modified binders, S5 and S6, respectively, have satisfactory ER results. Because all mixtures in the experiment had at least 15% RAP, it is unclear what effects RAP have on the ER results. The ER did provide a wide spread of results across the seven mixtures, and relative rankings for five of the seven mixtures followed expected trends. However, the predicted relative rankings of TDC resistance of the mixtures seem unlikely given the expected performance of S13 and N8. It will be interesting to see results of the mixtures after aging and how both aged and unaged results will compare to cracking on the test sections.

4.2 Texas Overlay Test

The Texas Overlay results are presented in Figure 24. The error bars in Figure 24 represent the sample standard deviation. It can be seen that TX-OT results for mixture S13 with GTR greatly exceeded the other six mixtures. In fact, the mean N_f of S13 was more than 28 times higher than all other mixtures. S13 is obviously different than the other six mixtures from a practical and statistical viewpoint. Mixture N8 with RAP/RAS failed at two cycles for each of the four replicates. This was not unexpected due to the extreme stiffness of this mixture. The results from mix S6 with polymer-modified asphalt (HiMA) were, however, very surprising. This mixture had a mean N_f that was lower than even the low density mix. In general, the relative rankings of the mixes using the TX-OT followed the expected trends with the exception of S6. It should be noted that all mixtures except S13 would fail the criteria of $N_f > 300$ for overlays according to Texas specifications.

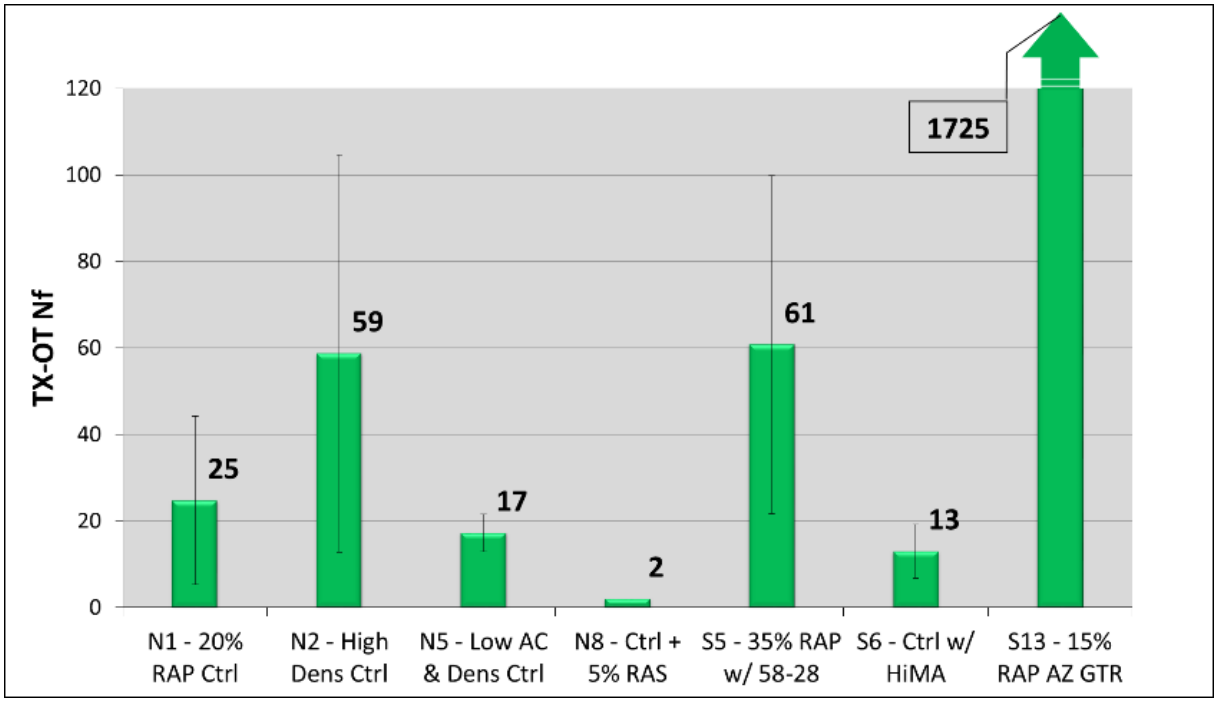

Figure 24: Texas Overlay Results.

Table 4 includes the coefficient of variation (CV) of each of the mixtures. The average CV for these seven sets of data was 45 percent. This value is in agreement with literature and past experience from other research studies using the OT conducted at NCAT (Ma, 2014; Tran, et al., 2012). Every replicate of N8 failed at the second cycle so the variance of this mixture was zero. From Table 4 it is clear that the variability of the data are very high. In fact, the mixture with the lowest CV (excluding N8), S13, actually had a standard deviation of eight times higher than the other mixtures but the high mean N_f resulted in the lowest CV. The high variability of the TX-OT could create problems if this test were to be selected as a TDC screening tool.

Table 4: Statistical Analysis of TX-OT Results.

Mix ID	Replicates	Average N_f	Standard Deviation	CV (%)
S13 - 15% RAP AZ GTR	4	1725	360	21
S5 - 35% RAP w/ 58-28	4	61	39	64
N2 - High Dens Ctrl	4	59	46	78
N1 - 20% RAP Ctrl	4	25	19	79
N5 - Low AC & Dens Ctrl	4	17	4	25
S6 - Ctrl w/ HiMA	3	13	6	48
N8 - Ctrl + 5% RAS	4	2	0	0

The results from Figure 24 were separated into tiers by assigning mixtures to tiers designated by numerals (I, II, III, etc.). Mixtures that share the same tier were believed to be statistically similar. Table 5 shows the resultant tiers. The very high variability in the mixtures, specifically N2 and S5, caused the t-tests to fail to determine significance between the middle five mixtures. N2 and S5 had much higher mean N_f than N5 and S6 but the extremely high variability caused the p-values to be too high to reject the null hypothesis that the mixtures were similar. More testing could possibly show the N2-N5, N2-S6, S5-N5, and S5-S6 comparisons to be a Type II error (fail to reject the null hypothesis when it should be rejected).

Table 5: Mixture tiers based on TX-OT results.

Mix ID	Mixture Tier
S13 - 15% RAP AZ GTR	I
S5 - 35% RAP w/ 58-28	II
N2 - High Dens Ctrl	
N1 - 20% RAP Ctrl	
N5 - Low AC & Dens Ctrl	
S6 - Ctrl w/ HiMA	
N8 - Ctrl + 5% RAS	III

Table 6 shows the p-values from the two sample t-tests for the TX-OT results at a 95% significance level. As shown in Table 6, none of the mixtures in Tier II were able to be distinguished from the others in terms of N_f. The high variability for the OT results of these

mixtures is the primary reason why no differences were statistically different. More samples could either reduce or confirm the variability and reduce the potential for Type II errors. As previously stated, it is assumed that S13 and N8 are significantly different from all other mixtures regardless of the resultant p-values because of the practical differences in these mixtures. There is evidence of practical differences between these two mixtures and the other mixtures. N8 is brittle and every replicate failed the TX-OT method at the minimum possible N_f and S13 had a N_f that is at least 28 times greater than the other mixtures. It is important to note that the low sample sizes used for the tests could have easily led to Type II errors.

Table 6: Two-sample t-tests of TX-OT p-values.

	N1	N2	N5	N8	S5	S6	S13
N1	-						
N2	0.245	-					
N5	0.507	0.17	-				
N8	0.102	0.09	0.006	-			
S5	0.174	0.95	0.113	0.057	-		
S6	0.34	0.144	0.387	0.093	0.095	-	
S13	0.003	0.003	0.002	0.002	0.003	0.002	-

Reject null hypothesis at $\alpha = 0.05$ (Mixtures are statistically different)

4.3 NCAT Modified Overlay Test

Figure 25 shows the results of the NCAT modified Overlay Test. The error bars in Figure 25 represent the sample standard deviation. As with the TX-OT results, mixture S13 with GTR was superior by a large margin and mixture N8 with RAP/RAS had the worst results. The results of the Texas method and NCAT method produced almost the same relative rankings. The only differences were the order of mixtures N5 with low density and S6 with polymer-modified

asphalt. Again, these relative rankings followed expected trends with the exception of S6 having a lower relative ranking than expected.

The variability of the results from the NCAT-OT method (listed in Table 7) is lower than the TX-OT method. The average CV for these seven sets of data was approximately 35 percent. However, it should be noted that the four of the seven mixtures had one specimen that failed the ASTM E178-08 outlier check. The lower CV's of the NCAT-OT method versus the TX-OT method might be misleading. Further research is needed to validate the NCAT-OT and to calibrate the results to field performance.

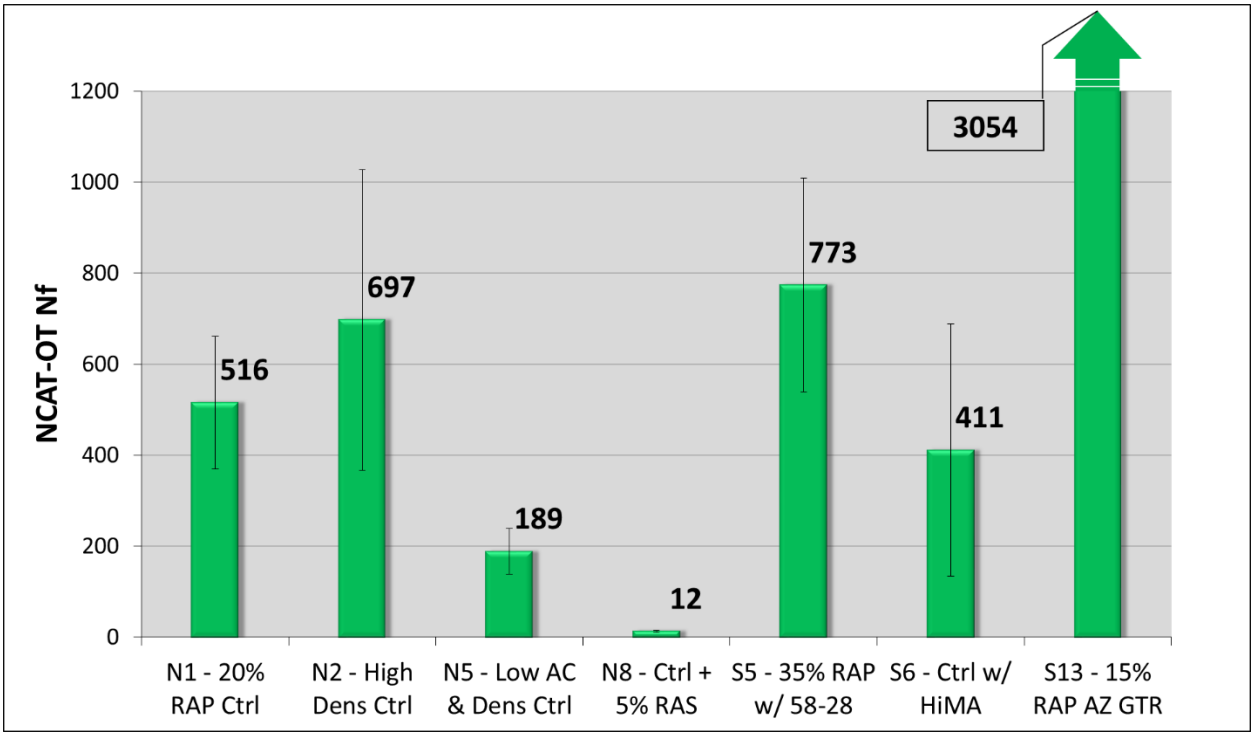

Figure 25: NCAT Overlay Results.

Table 7: Statistical Analyses of NCAT-OT Results.

Mix ID	Replicates	Average N_f	Standard Deviation	CV (%)
S13 - 15% RAP AZ GTR	3	3054	951	31
S5 - 35% RAP w/ 58-28	3	773	235	30
N2 - High Dens Ctrl	4	697	330	47
N1 - 20% RAP Ctrl	3	516	146	28
S6 - Ctrl w/ HiMA	4	411	278	68
N5 - Low AC & Dens Ctrl	4	189	189	27
N8 - Ctrl + 5% RAS	3	12	2	17

The results from Figure 25 were used to assign mixtures into tiers. Using the same procedure used in Section 4.2 Texas Overlay Test regarding the grouping of TX-OT data, the NCAT-OT data were grouped as shown in Table 8. Mixtures that share the same tier were believed to be statistically similar. The large amounts of variability in the NCAT-OT results created difficulties in organizing mixtures according to tiers. From Figure 25, it is clear that there are large differences regarding the comparisons of N1-N5, N2-N5, and N5-S5. However, due to the lack of a valid, robust statistical test to determine differences among more than two mixtures, all of these mixtures had to be combined into the same tier because they all were similar to mixture S6.

Table 8: Mixture tiers based on NCAT-OT results.

Mix ID	Mixture Tier
S13 - 15% RAP AZ GTR	I
N1 - 20% RAP Ctrl	II
S5 - 35% RAP w/ 58-28	
N2 - High Dens Ctrl	
S6 - Ctrl w/ HiMA	
N5 - Low AC & Dens Ctrl	
N8 - Ctrl + 5% RAS	III

Table 9 shows the p-values from the two sample t-tests performed on the NCAT-OT data at a 95% significance level. As was the case with the TX-OT testing, it is assumed that there is a high chance of Type II errors due to the small sample sizes of the mixtures. It is also assumed that N8 and S13 are different than all other mixtures due to practical differences regardless of statistical results. The t-test between N8 and S6 yielded a p-value of 0.131 but this is most likely due to the extremely high variability in mixture S6 and would likely be found to be significant with more samples. Furthermore, S13 N_f is at least four times greater than all of the mixtures and is only hindered from being found to be extremely significant by its high variability and sample size of three.

Table 9: Two-sample t-tests of NCAT-OT p-values.

	N1	N2	N5	N8	S5	S6	S13
N1	-						
N2	0.372	-					
N5	0.024	0.056	-				
N8	0.006	0.025	0.006	-			
S5	0.193	0.74	0.051	0.03	-		
S6	0.612	0.281	0.304	0.131	0.183	-	
S13	0.044	0.054	0.035	0.031	0.056	0.044	-

Reject null hypothesis at $\alpha = 0.05$ (Mixtures are statistically different)

Comparisons between N5 and N1, N2, and S5 are interesting. The p-values for the t-tests between N5-N2 and N5-S5 were just above 0.05. More testing would be required to determine if these mixtures are truly similar. It is worth noting that N5 was calculated as being different from N1 but not from N2 or S5 despite N2 and S5 having higher mean N_f than N1. This was due to the high variability and requires more testing to accurately determine true significance.

4.4 SCB-LTRC

Table 10 shows results of the average strain energy to failure of each notch depth for every mixture along with the corresponding CV. With one exception (S13 – 31.8 mm notch), all CVs were below 20% and the overall average of CV was approximately 10%. This CV was in agreement with values found in literature, is lower than what was determined for the OT results (Arabani & Ferdowsi, 2009). However, this was largely expected given that the OT is a cyclic fatigue test while the SCB is a monotonic strength test.

Table 10: SCB Testing Results

Mixture	Notch Length (mm)	Avg. U (Kn-mm)	Replicates	CV (%)
N1 - 20% RAP Ctrl	25.4	0.53	4	10%
	31.8	0.40	4	13%
	38.1	0.26	3	8%
N2 - High Dens Ctrl	25.4	0.76	3	2%
	31.8	0.49	3	5%
	38.1	0.32	4	9%
N5 - Low AC & Dens Ctrl	25.4	0.46	4	15%
	31.8	0.28	4	11%
	38.1	0.22	4	19%
N8 - Ctrl + 5% RAS	25.4	0.47	4	13%
	31.8	0.28	3	1%
	38.1	0.19	4	7%
S5 - 35% RAP w/ 58-28	25.4	0.47	4	12%
	31.8	0.33	4	8%
	38.1	0.23	4	17%
S6 - Ctrl w/ HiMA	25.4	0.49	4	5%
	31.8	0.34	4	9%
	38.1	0.23	4	6%
S13 - 15% RAP AZ GTR	25.4	0.81	3	3%
	31.8	0.61	4	21%
	38.1	0.46	4	12%

Table 11 lists the Jc results and the coefficient of determination for the dU/da slope for each of the mixtures. Note that mixtures N1, N5, S5, and S13 had R^2 values of less than 90%. These mixtures yielded larger error in the regression analysis of the slopes which led to larger estimations of the slope standard deviations. Figure 26 displays the results of the seven mixtures with error bars representing standard deviation of the Jc. The two mixtures with the highest Jc values were N2 with high density and S13 with GTR and were the only ones to meet the criterion recommended by LTRC (Cooper III, et al., 2016). However, the Jc values for this data set did not clearly distinguish between any of the mixtures expected to have medium to low TDC cracking resistance The mixture with polymer-modified binder, S6, was designed to be highly TDC resistant but the Jc of S6 was similar to the medium to low expected cracking sections. The SCB did have relatively low variability in the experiment but the inability of the test to distinguish between many of the mixtures with very different properties is a cause for concern. Obviously, field cracking results are required to validate the assumed TDC resistance of the mixtures.

Table 11: Jc Results and Coefficients of Determination

Mix ID	Jc (kJ/m^2)	Avg CV of Strain Energy	R^2 of dU/da
N2 - High Dens Ctrl	0.61	5%	0.973
S13 - 15% RAP AZ GTR	0.51	12%	0.791
N8 - Ctrl + 5% RAS	0.39	7%	0.917
S6 - Ctrl w/ HiMA	0.37	6%	0.966
N1 - 20% RAP Ctrl	0.36	10%	0.853
N5 - Low AC & Dens Ctrl	0.34	15%	0.813
S5 - 35% RAP w/ 58-28	0.34	12%	0.829

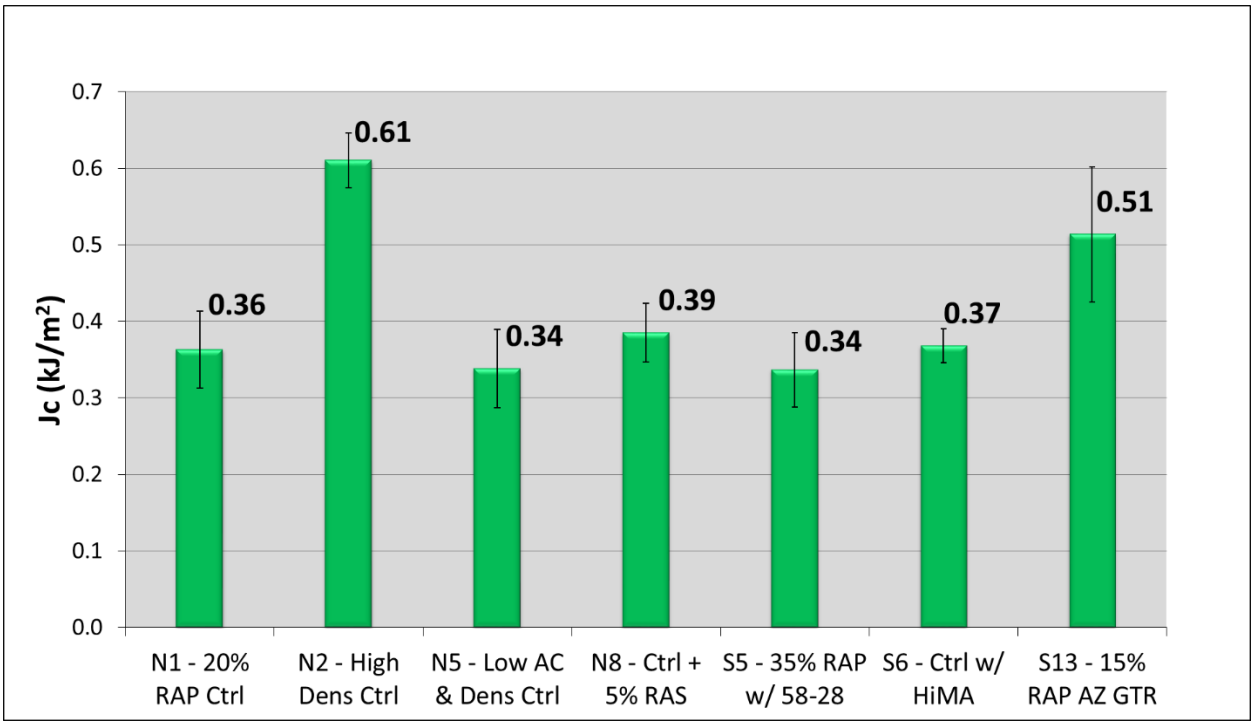

Figure 26: Jc Results from SCB Testing

In an effort to explore possible ways to reduce testing time, the results of the middle notch depth were removed from the analysis. The new Jc values from two notch depths were all less < 1% different than the Jc values from three notch depths. The results from this analysis are shown in Table 12. Other studies have indicated the importance of the middle notch depth (Mull, et al., 2002; Wu, Mohammad, Wang, & Mull, 2005), but the findings presented in this paper indicate the possibility of achieving a pass/fail criterion result with 33% less sample preparation and testing.

Table 12: Comparison of J_c results with two and three notch depths.

Mix ID	J_c (kJ/m^2) results with:		% change	Rank with:	
	3 notches	2 notches		3 notches	2 notches
N1 - 20% RAP Ctrl	0.363	0.367	-0.9%	5	5
N2 – High Dens Ctrl	0.610	0.614	-0.6%	1	1
N5 - Low AC & Dens Ctrl	0.338	0.336	0.7%	6	7
N8 - Ctrl + 5% RAS	0.385	0.383	0.5%	3	3
S5 - 35% RAP w/ 58-28	0.337	0.340	-0.8%	7	6
S6 - Ctrl w/ HiMA	0.368	0.367	0.3%	4	4
S13 - 15% RAP AZ GTR	0.514	0.515	-0.2%	2	2

As previously discussed in Section 3.7 Statistical Analyses, statistical analysis of differences between Jc results of mixtures was difficult due to limitations in the typical methods. The 95% confidence interval for each of the seven mixtures was calculated and used to determine statistically significant differences between mixtures. Figure 27 shows the absolute value of the dU/da slope of each mixtures and the whiskers represent the 95% confidence interval. Mixtures were considered different if their confidence intervals do not overlap.

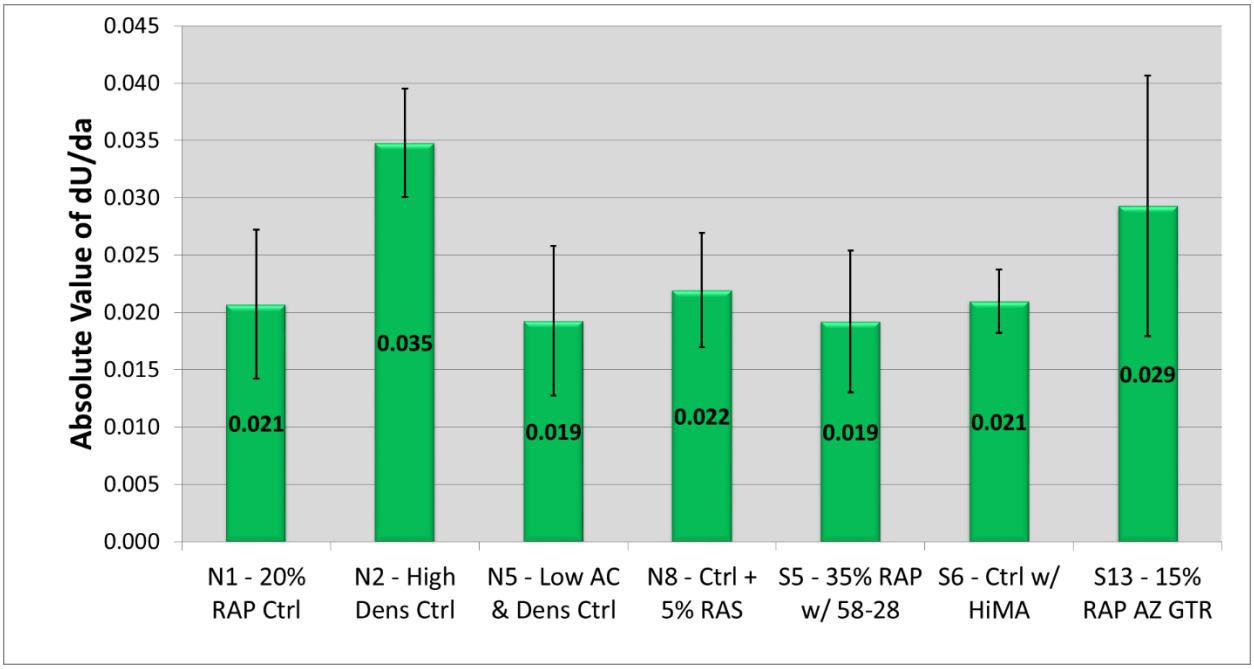

Figure 27: 95% Confidence Intervals for dU/da

Results from Figure 27 are summarized in tabular form in Table 13 using the same method discussed in Section 4.2 Texas Overlay Testregarding grouping the mixtures into tiers. In this case, if the confidence intervals of two mixtures overlap, they are assigned the same tier. It was not possible to perform t-tests on the Jc results to assess the validity of the proposed tiers because Jc is a single value and there are no replicates.

Table 13: Statistical grouping of SCB results

Mix ID	Mixture Tier
N2 - High Dens Ctrl	I
S13 - 15% RAP AZ GTR	
N8 - Ctrl + 5% RAS	II
S6 - Ctrl w/ HiMA	
N1 - 20% RAP Ctrl	
N5 - Low AC & Dens Ctrl	
S5 - 35% RAP w/ 58-28	

4.5 IFIT

Figure 28 shows the results of the IFIT and the error bars represent sample standard deviation. For each mixture, a minimum of six replicates were tested before the outlier analysis was performed. As with several other tests, S13 had the best result and N8 the worst result for the IFIT test. These two mixes also had the highest and lowest variance, respectively. Counter to the expected trend, the low density mixture, N5, had a higher mean FI than the high density mixture, N2. Table 14 lists the FI values of each mix and the corresponding variability. The FI results have much lower variability than the OT methods which bodes well for its potential usage as a specification criterion. Again, this trend was largely expected for the monotonic tests in comparison with the cyclic OT. The average CV for these seven sets of IFIT data was approximately 18 percent. However, it should be noted that only the mixture S13 would have the preliminary FI pass/fail criterion of 8 set forth by the Illinois DOT.

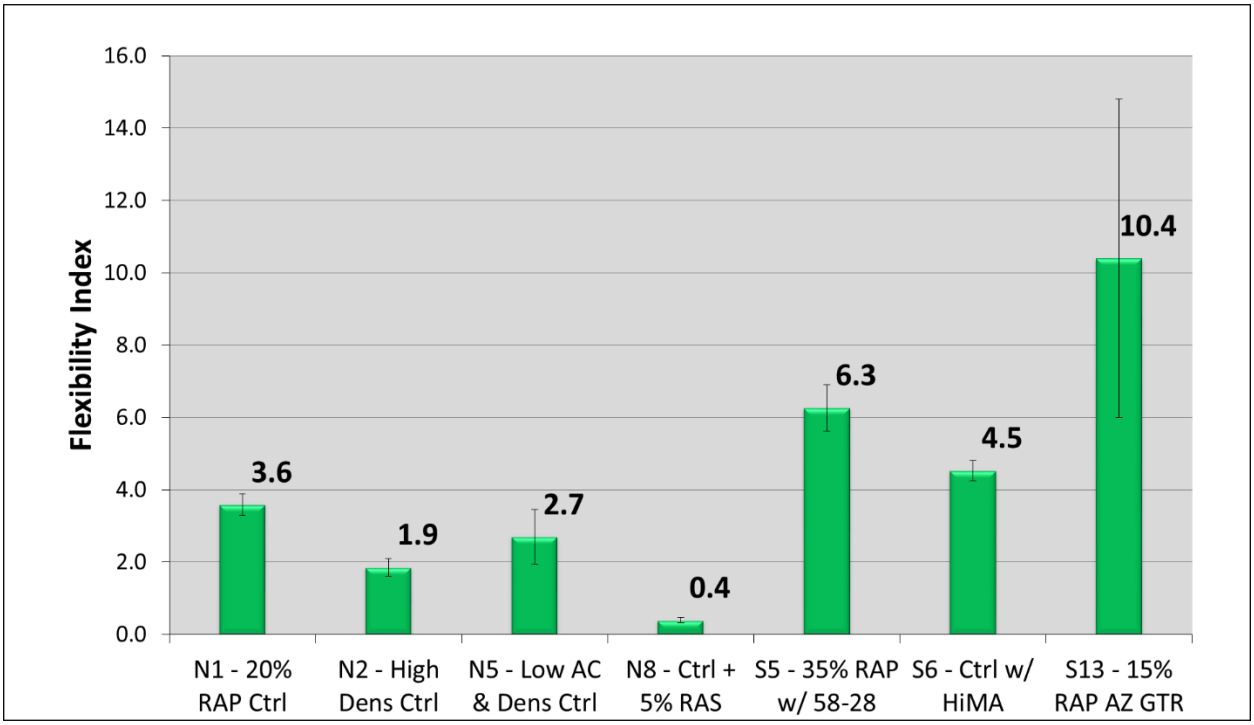

Figure 28: IFIT Results

Table 14: Statistical Analysis of IFIT Results

Mix ID	Replicates	Average FI	Standard Deviation	CV (%)
S13 - 15% RAP AZ GTR	6	10.4	4.4	42
S5 - 35% RAP w/ 58-28	6	6.3	0.6	10
S6 - Ctrl w/ HiMA	5	4.5	0.3	6
N1 - 20% RAP Ctrl	7	3.6	0.3	8
N5 - Low AC & Dens Ctrl	6	2.7	0.8	29
N2 - High Dens Ctrl	5	1.9	0.2	13
N8 - Ctrl + 5% RAS	9	0.4	0.1	18

The results of Figure 28 are summarized into Table 15 using the previously discussed method of grouping mixture results. The IFIT certainly had the largest spread of results of any of the cracking tests. The combination of the spread of means with relatively low standard deviations provides the opportunity to better distinguish between mixture testing results. Table 15 shows that five mixtures were assigned to tiers in which they were the only member. Mixtures S5 and

S13 were assigned the same tier because the low end of the S13 standard deviation was low enough to overlap with S5.

Table 15: Statistical grouping of IFIT results.

Mix ID	Mixture Tier
S13 - 15% RAP AZ GTR	I
S5 - 35% RAP w/ 58-28	
S6 - Ctrl w/ HiMA	II
N1 - 20% RAP Ctrl	III
N5 - Low AC & Dens Ctrl	IV
N2 - High Dens Ctrl	V
N8 - Ctrl + 5% RAS	VI

Table 16 shows the p-values from the two-sample t-tests of the IFIT results at a significance level of 0.05. The wide spread of FI values and the relatively low standard deviations caused every comparison except one to yield a significant p-value. The only comparison to not result in a significant difference was the comparison between S13 and S5, which were the two top performers in IFIT testing. More testing is required to determine if this is a Type II error due to high variability in S13 or if these mixtures are truly statistically similar.

Table 16: Two-sample t-tests of IFIT p-values.

	N1	N2	N5	N8	S5	S6	S13
N1	-						
N2	0.000	-					
N5	0.037	0.046	-				
N8	0.000	0.000	0.001	-			
S5	0.000	0.000	0.000	0.000	-		
S6	0.000	0.000	0.002	0.000	0.001	-	
S13	0.013	0.005	0.008	0.003	0.072	0.023	-

Reject null hypothesis at $\alpha = 0.05$ (Mixtures are statistically different)

4.6 Summary of All Testing Results

Table 17 lists the relative rankings from each of the five cracking tests. The performance of each mixture on the five cracking tests were ranked individually and the average ranking of the five tests was calculated. The mixtures are presented in Table 17 in order of average relative rank. Presenting the mixtures in order of statistical groupings would have led to confusing or misleading results because there was no simple way to compare statistical test groups to the numerical rankings of the Energy Ratio test that yielded reliable final rankings. The following observations may be made from Table 17:

- Mixture S13, with a high GTR-modified binder content, had the highest ranking by the OT methods and IFIT, second highest ranking by SCB, but the lowest ER. Practical differences between S13 and the other mixtures, namely the GTR binder, the high total binder content, larger NMAS, and gap-gradation caused this mixture to behave much differently than the other mixtures.
- The high density mixture, N2, had a fairly high ranking for all of the tests except for the IFIT.
- Mixture S5 with 35% RAP and PG 58-28 binder was ranked second highest by both OT methods and the IFIT, but was ranked lowest by the SCB test and near the middle by ER. However, the mixtures with the five lowest Jc results in the SCB test had similar Jc values.
- Mixture S6, which contained a binder with a high polymer content, was ranked differently by each test.
- The control mixture, N1, had results near the middle of the group in every test as expected.

- Mixture N8, which contained RAS had the highest ER but had worst results in both OT methods and the IFIT. SCB results for this mixture were ranked third although the mixtures with the five lowest Jc results in SCB testing were similar. The high ER result was due to the extremely low creep rate exhibited by this very stiff mixture. For aged specimens, N8 may not pass the minimum $DCSE_{HMA}$ criterion for ER testing.
- N5, designed with a low asphalt content (0.5% below optimum) and low target in-place density, was ranked similarly by all tests near the bottom of the order.

Table 17: Relative Rankings of the Results of the Cracking Tests

Mix ID	ER	OT - TX	OT - NCAT	IFIT	SCB	Average Ranking
S13 - 15% RAP AZ GTR	7	1	1	1	2	2.4
N2 - High Dens Ctrl	3	3	3	6	1	3.2
S5 - 35% RAP w/ 58-28	4	2	2	2	7	3.4
S6 - Ctrl w/ HiMA	2	5	6	3	4	4.0
N1 - 20% RAP Ctrl	5	4	4	4	5	4.4
N8 - Ctrl + 5% RAS	1	7	7	7	3	5.0
N5 - Low AC & Dens Ctrl	6	6	5	5	6	5.6

Table 18 includes a summary of the advantages and disadvantages of each laboratory cracking test relative to each other and accounts for the results of the experiment described in this thesis. This list is representative of the procedures described in this thesis only. It should be noted that some of these tests can be performed on alternative equipment. The relative costs of the tests are skewed because the ER requires highly sophisticated equipment to capture test data so this test has the highest relative cost. An AMPT was utilized for both OT methods, although the Texas method could be performed on a standalone device. The SCB cost refers to the test setup using an AMPT, however, there are numerous devices that are suitable for this test. An AMPT was chosen for this experiment to reduce variability and machine compliance. Testing times are estimates beginning from initiation of the reheating of plant mix in a bucket and ending with the

final test result. These times could be different for other aging conditions or applications. Finally, feasability refers to specimen preparation, testing, and data analysis and interpretation. The ER and both OT methods require gluing and extra instrumentation so these tests have lower simplicity rankings than the IFIT and SCB. The ER requires more instrumentation and specialized software than the other four tests so this test is designated as the most complex.

Table 18: Advantages and disadvantages of each laboratory cracking test.

Test Method	Advantage	Disadvantage
Energy Ratio	Holistic approach to TDC Developed specifically for TDC assessment Calibrated using real pavement conditions in Florida	Expensive equipment required (Servo-hydraulic device, temperature controlled) Extensive sample preparation and testing time required (4-5 days) Limited range of validated application No measurement of variability Results for high and low stiffness mixtures are questionable
Texas Overlay Test	Commonly used to assess crack resistance Simple data analysis Replicates produced	High variability Cracking mechanism different from TDC Gluing requires extra day to total sample prep and testing time (3-4 days)
NCAT Overlay Test	Lower variability than TX-OT Simple data analysis Replicates produced	High variability Cracking mechanism different from TDC Gluing requires extra day to total sample prep and testing time (3-4 days) Limited number of studies Must use an AMPT
SCB	Shortest testing time (2-3 days) Commonly used to assess crack resistance Replicates produced Low variability	Large number of samples required Inconsistent spread of results AMPT device is expensive (optional)
IFIT	Lowest relative cost Shortest testing time (2-3 days) Good spread of results Simple data analysis Replicates produced Low variability	Limited number of studies Did not capture effects of high density

CHAPTER 5 – CONCLUSIONS AND RECOMMENDATIONS

This study compared the results of five popular asphalt mixture cracking tests on a unique set of seven experimental plant-produced mixtures designed to have a wide range of cracking susceptibilities. Overall, the five tests ranked the mixes differently. Based on the data presented herein on the reheated plant-produced, lab-compacted samples, the following conclusions are recommendations are made:

- The Energy Ratio testing results ranked the mixtures in accordance with their anticipated performance for five of the seven mixtures. However, it ranked the mixture expected to have very good field performance, S13 (15% RAP AZ GTR), last and a mixture expected to have poor field performance, N8 (Control + 5% RAS), first. This was largely driven by the creep compliance values for these two mixtures.
- The current Energy Ratio criteria may not be appropriate for reheated plant mixtures. More research is needed to evaluate ER for reheated plant mix or short-term aged specimens. Also, further validation is needed for mixtures with very high $DCSE_{HMA}$. Equipment cost and test complexity will need to be reduced before the ER can be fully implemented in the industry as a TDC screening test.
- The OT results (both Texas method and NCAT-modified method) ranked the mixtures largely in accordance with their anticipated level of field cracking. Results for the 20% RAP mix with highly modified asphalt (HiMA) from Section S6 did not fall in line with anticipated field performance. The OT cycles to failure by both methods for this mix were generally low while the mix is expected to perform well.
- The CV for the Texas method and NCAT-modified OT were approximately 45% and 35%, respectively. While the NCAT-modified OT produced somewhat lower variability, the

variability for both data sets were consistent with experience and published values. This does not necessarily indicate that either OT method should not be used for analysis of TDC but the results of this study show that the cyclic tests had greater variability than the monotonic loading tests. Furthermore, the extra time required to glue OT specimens causes the overall testing time to be greater than the two monotonic tests.

- The SCB test indicated that mixtures N2 (high density) and S13 (GTR) were most resistant to TDC. However, the SCB was unable to discern differences among the other mixtures. The remaining five mixtures all produced Jc values within 0.05 kJ/m^2 of each other. An AMPT was used for SCB testing in this study. However, on a different loading device, the SCB cost could be reduced. Data analysis for this method is easily automated in a spreadsheet.
- The IFIT produced a large spread of flexibility index results among the seven mixtures and produced the expected ranking for mixtures N5 (Control + low AC & density), N8 (Control + 5% RAS), S6 (Control with HiMA), and S13 (15% RAP AZ GTR). N2 (Control + high density), however, was not ranked as predicted, with the mean FI of the low density mixture higher than that of the high density mixture. The IFIT has the lowest cost and testing time of the five cracking tests in the experiment. All data analyses are performed using provided software and the output is easily interpreted and reported.
- The CV of both the SCB Jc and IFIT FI were 10% and 18%, respectively. These values were consistent with values found in literature. Both of these tests apply a monotonic loading and had better repeatability than the cyclic OT.

As of October 2016, over 4.3 million ESAL's had been applied to the mixtures on the NCAT Test Track and no visible cracking had occurred. As the experiment progresses and TDC occurs, the results of this study will be combined with others to analyze the suitability of each of the five

tests to predict TDC in a mix design application. The suitability of each test will be determined based on lab-field correlations, testing variability, costs, and test feasibility.

REFERENCES

AASHTO. (2011). AASHTO Designation: T 322-07. Standard Method of Test for Determining the Creep Compliance and Strength of Hot Mix Asphalt (HMA) Using the Indirect Tensile Test Device. American Association of State Highway and Transportation Officials.

Al-Qadi, I. L., Ozer, H., Lambros, J., El Khatib, A., Singhvi, P., Khan, T., . . . Doll, B. (2015). Testing protocols to ensure performance of high asphalt binder replacement mixes using RAP and RAS. Urbana-Champaign, Illinois: Illinois Center for Transportation.

Arabani, M., & Ferdowsi, B. (2009, February). Evaluating the Semi-Circular Bending Test for HMA Mixtures. IJE Transactions A: Basics, Vol. 22(No. 1), 47-58.

ASTM International. (2011). ASTM Designation D7369-11. Standard Test Method for Determining the Resilient Modulus of Bituminous Mixtures by Indirect Tension Test. West Conshohocken, PA.

ASTM International. (2012). ASTM Designation D6931-12. Standard Test Method for Indirect Tensile (IDT) Strength of Bituminous Mixtures. West Conshohocken, PA.

ASTM International. (2008). ASTM Designation E178-08. Standard Practice for Dealing with Outlying Observations. West Conshohocken, PA.

Bennert, T. (2009). Lab overlay tester for characterizing HMA crack resistance. 2009 Northeast Asphalt User Producer Group. South Portland, Maine: NEAUPG.

Bennert, T., & Maher, A. (2008). Field and Laboratory Evaluation of a Reflective Crack Interlayer in New Jersey. Transportation Research Record: Journal of the Transportation Research Board, No. 2084, 114-123.

Chong, K. P., & Kuruppu, M. D. (1988). New Specimens for Mixed Mode Fracture Investigations of Geomaterials. Engineering Fracture Mechanics, Vol. 30(No. 5), 701-712.

Cooper III, S. B., King, W., & Kabir, M. S. (2016). Testing and analysis of LWT and SCB properties of asphalt concrete mixtures. Baton Rouge, Louisiana: Louisiana Transportation Research Center. Retrieved from http://www.ltrc.lsu.edu/pdf/2016/FR_536.pdf

de Freitas, E. F., Pereira, P., Picado-Santos, L., & Papagiannakis, A. T. (2005). Effect of Construction Quality, Temperature, and Rutting on Initiation of Top-Down Cracking. Transportation Research Record: Journal of the Transportation Research Board, No. 1929, 174-182.

Devore, J., & Farnum, N. (2005). Applied Statistics for Engineers and Scientists (Second Edition). Belmont, CA: Thomson Brooks/Cole.

Gerritsen, A. H., van Gurp, C. P., van der Heidi, J. J., Molenaar, A. A., & Pronk, A. C. (1987). Prediction and prevention of surface cracking in asphaltic pavements. Sixth International Conference on Structural Design of Asphalt Pavements Vol. 1 (pp. 378-391). Ann Arbor, Michigan: The University of Michigan.

Harmelink, D., Shuler, S., & Aschenbrener, T. (2008). Top-Down Cracking in Asphalt Pavements: Causes, Effects, and Cures. Journal of Transportation Engineering - ASCE, 1-6.

Hosford, W. F. (2005). Mechanical Behavior of Materials. New York: Cambridge University Press.

Huang, L., Cao, K., & Zeng, M. (2009). Evaluation of Semicircular Bending Test for Determining Tensile Strength and Stiffness Modulus of Asphalt Mixtures. ASTM: Journal of Testing and Evaluation, Vol. 37(No. 2), 1-7.

Hugo, F., & Kennedy, T. W. (1985). Surface cracking of asphalt mixtures in southern Africa. Journal of the Association of Asphalt Paving Technologists, 454-501.

Illinois Department of Transportation. (2015). Illinois Flexibility Index Test - Pilot Projects. Springfield, Illinois: IDOT. Retrieved from http://www.idot.illinois.gov/Assets/uploads/files/Transportation-System/Bulletins-&-Circulars/Bureau-of-Local-Roads-and-Streets/Circular-Letters/Informational/CL2015-19.pdf

IPC Global. (2012). AMPT Overlay Test Kit. Retrieved from IPC Global: http://instrotek.com/wordpress/wp-content/uploads/AMPT-Overlay-Test-Kit.pdf

Kim, M., Mohammad, L. N., & Elsefi, M. A. (2012). Characterization of Fracture Properties of Asphalt Mixtures as Measured by Semicircular Bend Test and Indirect Tension Test. Transportation Research Record: Journal of the Transportation Research Board, No. 2296, 115-124.

Li, X., & Marasteanu, M. (2004). Evaluation of the Low Temperature Fracture Resistance of Asphalt Mixtures Using the Semi Circular Bend Test. Journal of the Association of Asphalt Paving Technologists, Vol. 73, 401-426.

Ma, W. (2014). Proposed Improvements to Overlay Test for Determining Cracking Resistance of Asphalt Mixtures. Auburn University, Department of Civil Engineering. Auburn, AL: Auburn University.

Matsuno, S., & Nishizawa, T. (1992). Mechanism of Longitudinal Surface Cracking in Asphalt Pavement. Proceedings of the 7th International Conference on Asphalt Pavements, Vol. 2 (pp. 277-291). The University of Nottingham.

Molenaar, A. A., Scarpas, A., Liu, X., & Erkens, S. J. (2002). Semi-Circular Bending Test; Simple but Useful? Journal of the Association of Asphalt Paving Technologists, 794-815.

Mull, M. A., Stuart, K., & Yehia, A. (2002). Fracture Resistance Characterization of Chemically Modified Crumb Rubber Asphalt Pavement. Journal of Materials Science, Vol. 37, 557-566.

Myers, L. A. (2000). Development and Propagation of Surface-Initiated Longitudinal Wheel Path Cracking in Flexible Highway Pavements. Gainesville, FL: University of Florida.

Myers, L. A., Roque, R., & Ruth, B. E. (1998). Mechanisms of surface-initiated longitudinal wheel path cracks in high-type bituminous pavements. Journal of the Association of Asphalt Paving Technologists, 401-432.

Ozer, H., Al-Qadi, I. L., Lambros, J., El-Khatib, A., Singhvi, P., & Doll, B. (2016a). Development of fracture-based flexibility index for asphalt concrete cracking potential using modified semi-circle bending test parameters. Construction and Building Materials 115, 390-401.

Ozer, H., Al-Qadi, I. L., Singhvi, P., Khan, T., Rivera-Perez, J., & El-Khatib, A. (2016b). Fracture Characterization of Asphalt Mixtures with RAP and RAS Using the Illinois Semi-Circular Bending Test Method and Flexibility Index. Proceedings of the 95th Annual Meeting of the Transportation Research Board.

Pellinen, T., Rowe, G., & Biswas, K. (2004). Evaluation of Surface (Top-Down) Longitudinal Wheel Path Cracking. West Lafayette: Purdue University.

Roque, R., Birgisson, B., Drakos, C., & Dietrich, B. (2004). Development and Field Evaluation of Energy-Based Criteria for Top-down Cracking Performance of Hot Mix Asphalt. Journal of the Association of Asphalt Paving Technologists, Vol. 73, 229-260.

Roque, R., Buttlar, W. G., Ruth, B. E., Tia, M., Dickison, S. W., & Reid, B. (1997). Evaluation of SHRP indirect tension tester to mitigate cracking in asphalt concrete pavements and overlays. Gainesville, Florida: University of Florida.

Roque, R., Kim, R. Y., Baek, C., Thirunavukkarasu, S., Underwood, B. S., & Guddati, M. N. (2010). NCHRP Web-Only Document 162: Top-down cracking of hot-mix asphalt layers: Models for initiation and propagation. Washington, D.C.: Transportation Research Board of the National Academies.

Rowe, G. M., & Bouldin, M. G. (2000). Improved techniques to evaluate the fatigue resistance of asphaltic mixtures. Proceedings of the 2nd Eurasphalt & Eurobitume Congress Barcelona 2000. Barcelona, Spain.

Sheehy, E. (2013, March 6). Case Study: High RAP Pilot Project. Presentation from the New Jersey Asphalt Paving Conference. Retrieved July 28, 2016, from https://cait.rutgers.edu/system/files/u10/High_RAP_NJDOT_--_Sheehy.pdf

Shu, X., Huang, B., & Vukosavljevic, D. (2008). Laboratory evaluation of fatigue characteristics of recycles asphalt mixture. Construction and Building Materials 22, 1323-1330.

Timm, D. H., Sholar, G. A., Kim, J., & Willis, J. R. (2009). Forensic Investigation and Validation of Energy Ratio Concept. Transportation Research Record: Journal of the Transportation Research Board, No. 2127, 43-51.

Tran, N., Taylor, A., & Willis, J. R. (2012). Effect of rejuvenator on performance properties of HMA mixtures with high RAP and RAS contents. Auburn, AL: National Center for Asphalt Technology.

TxDOT. (2014, February). TxDOT Designation: Tex-248-F. Test Procedure for Overlay Test. Construction Division.

Uhlmeyer, J. S., Willoughby, K., Pierce, L. M., & Mahoney, J. P. (2000). Top-Down Cracking in Washington State Asphalt Concrete Wearing Courses. Transportation Research Record: Journal of the Transportation Research Board, No. 1730, 110-116.

Walubita, L. F., Faruk, A. N., Das, G., Tanvir, H. A., Zhang, J., & Scullion, T. (2012). The Overlay Tester: A sensitivity study to improve repeatability and minimize variability in the test results. College Station, TX: Texas Transportation Institute.

Wang, J., Birgisson, B., & Roque, R. (2007). Windows-Based Top-Down Cracking Design Tool for Florida Using Energy Ratio Concept. Transportation Research Record: Journal of the Transportation Research Board, No. 2037, 86-96.

Wen, H., & Bhusal, S. (2015). Development of Phenomenological Top-Down Cracking Initiation Model for Mechanistic-Empirical Pavement Design. Transportation Research Record: Journal of the Transportation Research Board, No. 2474, 12-18.

Willis, J. R., Taylor, A. J., & Nash, T. M. (2016). Laboratory and Field Evaluation of Florida Mixtures at the 2012 National Center for Asphalt Technology Pavement Test Track. Transportation Research Record: Journal of the Transportation Research Board, No. 2590, 65-73.

Willis, R., Timm, D., West, R., Powell, B., Robbins, M., Taylor, A., . . . Bianchini, A. (2009). NCAT Report 09-08: Phase III NCAT Test Track Findings. Auburn, AL: National Center for Asphalt Technology.

Wu, Z., Mohammad, L. N., Wang, L. B., & Mull, M. A. (2005). Fracture Resistance Characterization of Superpave Mixtures Using the Semi-Circular Bending Test. Journal of ASTM International, Vol. 2(No. 3), Paper ID JAI12264 [online].

Zhang, Z., Roque, R., Birgisson, B., & Sangpetgnam, B. (2001). Identification and Verification of a Suitable Crack Growth Law for Asphalt Mixtures. Journal of the Association of Asphalt Paving Technologists, Vol. 70, 206-241.

Zhou, F., & Scullion, T. (2005). Overlay Tester: A rapid performance related crack resistance test. College Station, TX: Texas Transportation Institute.

Zhou, F., Hu, S., & Scullion, T. (2009). Overlay Tester: A simple and rapid test for HMA Fracture Property. Proceedings of the 2009 Geohunan International Conference. Hunan, P.R. China.

Zhou, F., Hu, S., Chen, D.-H., & Scullion, T. (2007). Overlay Tester: Simple performance test for fatigue cracking. Transportation Research Record: Journal of the Transportation Research Board, No. 2001, 1-8

APPENDIX A – MIXTURE PROPERTIES AND TEST SECTION INFORMATION

5/23/2016

Quadrant: N
Section: 1
Sublot: 1

Laboratory Diary

General Description of Mix and Materials

Design Method:	Super
Compactive Effort:	80 gyrations
Binder Performance Grade:	67-22
Modifier Type:	NA
Aggregate Type:	Granite/Sand/RAP
Design Gradation Type:	DGA

Avg. Lab Properties of Plant Produced Mix

Sieve Size	Target	QC
25 mm (1"):	100	100
19 mm (3/4"):	100	100
12.5 mm (1/2"):	100	99
9.5 mm (3/8"):	99	97
4.75 mm (#4):	74	67
2.36 mm (#8):	51	52
1.18 mm (#16):	39	41
0.60 mm (#30):	26	28
0.30 mm (#50):	15	15
0.15 mm (#100):	9	9
0.075 mm (#200):	6.2	5.4
Binder Content (Pb):	5.7	5.4
Eff. Binder Content (Pbe):	5.0	4.7
Dust-to-Eff. Binder Ratio:	1.2	1.1
RAP Binder Replacement (%):	19.1	17.7
RAS Binder Replacement (%):	0.0	0.0
Total Binder Replacement (%):	19.1	17.7
Rice Gravity (Gmm):	2.474	2.469
Bulk Gravity (Gmb):	2.375	2.375
Air Voids (Va):	4.0	3.8
Agg. Bulk Gravity (Gsb):	2.654	2.63
VMA:	15.6	15
VFA:	75	74

Construction Diary

Relevant Conditions for Construction

Completion Date:	August 5, 2015
24 Hour High Temperature (F):	97
24 Hour Low Temperature (F):	71
24 Hour Rainfall (in):	0.00
Planned Subot Lift Thickness (in):	1.5
Paving Machine:	Roadtec

Plant Configuration and Placement Details

Component	% Setting
Binder Content (Plant Setting)	5.8
89 Granite	39.0
Coarse Sand	25.0
M10 Granite	16.0
EAP -1/2 RAP	20.0
Evotherm P15	0.5

As-Built Sublot Lift Thickness (in):	1.6
Total Thickness of All New Sublots (in):	7.0
Approx. Underlying HMA Thickness (in):	5.5
Type of Tack Coat Utilized:	NTSS-1HM
Undilluted Target Tack Rate (gal/sy):	0.10
Approx. Avg. Temperature at Plant (F):	320
Avg. Measured Mat Compaction:	93.6%

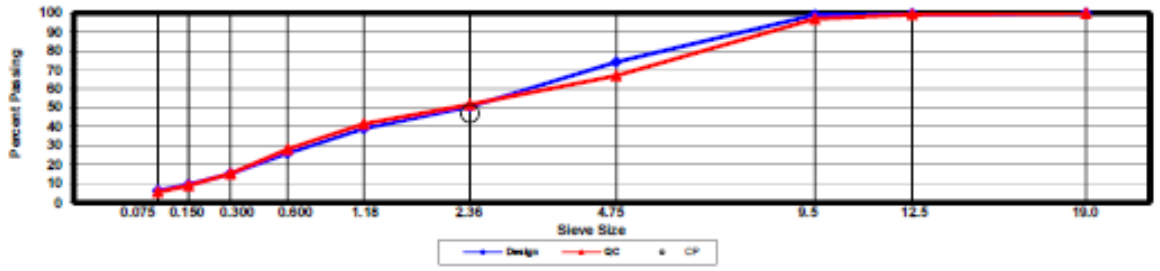

General Notes:
- References are by quadrant (E=East, N=North, W=West, S=South, L=Lee Rd 159, U=US-280), section #, and sublot (top=1).
- DGA, SMA, & OGFC refer to dense graded asphalt, stone matrix asphalt, & open-graded friction course, respectively.
- Production Gsb estimated using the actual production Gse and the difference between Gse and Gsb in the mix design.

Section and/or Sublot Specific Notes:
NA

5/23/2016

Quadrant: N
Section: 2
Sublot: 1

Laboratory Diary

General Desccription of Mix and Materials

Design Method:	Super
Compactive Effort:	80 gyrations
Binder Performance Grade:	67-22
Modifier Type:	NA
Aggregate Type:	Granite/Sand/RAP
Design Gradation Type:	DGA

Avg. Lab Properties of Plant Produced Mix

Sieve Size	Target	QC
25 mm (1"):	100	100
19 mm (3/4"):	100	100
12.5 mm (1/2"):	100	100
9.5 mm (3/8"):	99	98
4.75 mm (#4):	74	70
2.36 mm (#8):	51	54
1.18 mm (#16):	39	43
0.60 mm (#30):	26	28
0.30 mm (#50):	15	15
0.15 mm (#100):	9	9
0.075 mm (#200):	6.2	5.6
Binder Content (Pb):	5.7	5.4
Eff. Binder Content (Pbe):	5.0	4.7
Dust-to-Eff. Binder Ratio:	1.2	1.2
RAP Binder Replacement (%):	19.1	17.9
RAS Binder Replacement (%):	0.0	0.0
Total Binder Replacement (%):	19.1	17.9
Rice Gravity (Gmm):	2.474	2.468
Bulk Gravity (Gmb):	2.375	2.372
Air Voids (Va):	4.0	3.9
Agg. Bulk Gravity (Gsb):	2.654	2.63
VMA:	15.6	15
VFA:	75	73

Construction Diary

Relevant Conditions for Construction

Completion Date:	August 5, 2015
24 Hour High Temperature (F):	97
24 Hour Low Temperature (F):	71
24 Hour Rainfall (in):	0.00
Planned Subot Lift Thickness (in):	1.5
Paving Machine:	Roadtec

Plant Configuration and Placement Details

Component	% Setting
Binder Content (Plant Setting)	5.8
89 Granite	39.0
Coarse Sand	25.0
M10 Granite	16.0
EAP -1/2 RAP	20.0
Evotherm P15	0.5

As-Built Sublot Lift Thickness (in):	1.5
Total Thickness of All New Sublots (in):	6.7
Approx. Underlying HMA Thickness (in):	5.2
Type of Tack Coat Utilized:	NTSS-1HM
Undiluted Target Tack Rate (gal/sy):	0.10
Approx. Avg. Temperature at Plant (F):	320
Avg. Measured Mat Compaction:	96.1%

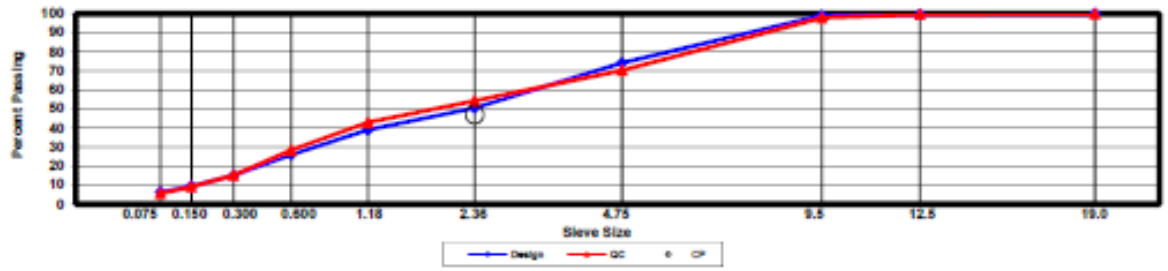

General Notes:
- References are by quadrant (E=East, N=North, W=West, S=South, L=Lee Rd 159, U=US-280), section #, and sublot (top=1).
- DGA, SMA, & OGFC refer to dense graded asphalt, stone matrix asphalt, & open-graded friction course, respectively.
- Production Gsb estimated using the actual production Gse and the difference between Gse and Gsb in the mix design.

Section and/or Sublot Specific Notes:
NA

5/23/2016

Quadrant: N
Section: 5
Sublot: 1

Laboratory Diary

General Description of Mix and Materials

Design Method:	Super
Compactive Effort:	80 gyrations
Binder Performance Grade:	67-22
Modifier Type:	NA
Aggregate Type:	Granite/Sand/RAP
Design Gradation Type:	DGA

Avg. Lab Properties of Plant Produced Mix

Sieve Size	Target	QC
25 mm (1"):	100	100
19 mm (3/4"):	100	100
12.5 mm (1/2"):	100	100
9.5 mm (3/8"):	99	99
4.75 mm (#4):	74	73
2.36 mm (#8):	51	54
1.18 mm (#16):	39	42
0.60 mm (#30):	26	28
0.30 mm (#50):	15	15
0.15 mm (#100):	9	9
0.075 mm (#200):	6.2	5.7
Binder Content (Pb):	5.2	5.1
Eff. Binder Content (Pbe):	4.5	4.4
Dust-to-Eff. Binder Ratio:	1.4	1.3
RAP Binder Replacement (%):	20.9	18.9
RAS Binder Replacement (%):	0.0	0.0
Total Binder Replacement (%):	20.9	18.9
Rice Gravity (Gmm):	2.493	2.478
Bulk Gravity (Gmb):	2.355	2.348
Air Voids (Va):	5.5	5.3
Agg. Bulk Gravity (Gsb):	2.654	2.63
VMA:	15.9	15
VFA:	65	66

Construction Diary

Relevant Conditions for Construction

Completion Date:	July 24, 2015
24 Hour High Temperature (F):	89
24 Hour Low Temperature (F):	73
24 Hour Rainfall (in):	0.83
Planned Subot Lift Thickness (in):	1.5
Paving Machine:	Roadtec

Plant Configuration and Placement Details

Component	% Setting
Binder Content (Plant Setting)	5.1
89 Granite	39.0
Coarse Sand	25.0
M10 Granite	16.0
EAP -1/2 RAP	20.0
Evotherm P15	0.5
As-Built Sublot Lift Thickness (in):	1.3
Total Thickness of All New Sublots (in):	6.1
Approx. Underlying HMA Thickness (in):	4.8
Type of Tack Coat Utilized:	NTSS-1HM
Undiluted Target Tack Rate (gal/sy):	0.10
Approx. Avg. Temperature at Plant (F):	320
Avg. Measured Mat Compaction:	90.3%

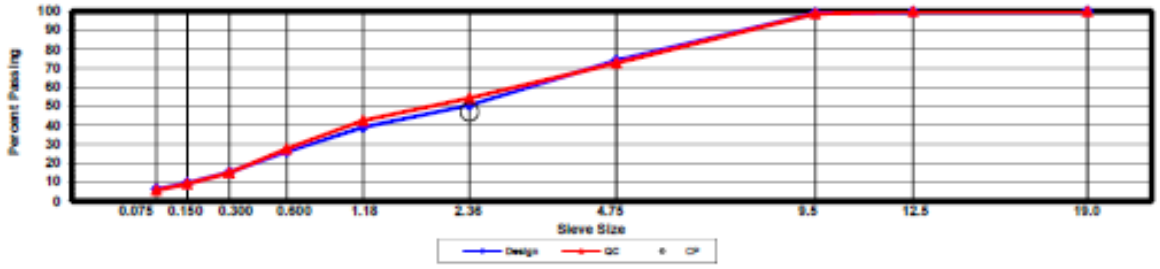

General Notes:
- References are by quadrant (E=East, N=North, W=West, S=South, L=Lee Rd 159, U=US-280), section #, and sublot (top=1).
- DGA, SMA, & OGFC refer to dense graded asphalt, stone matrix asphalt, & open-graded friction course, respectively.
- Production Gsb estimated using the actual production Gse and the difference between Gse and Gsb in the mix design.

Section and/or Sublot Specific Notes:
NA

5/23/2016

Quadrant: N
Section: 8
Sublot: 1

Laboratory Diary

General Desccription of Mix and Materials

Design Method:	Super
Compactive Effort:	80 gyrations
Binder Performance Grade:	67-22
Modifier Type:	NA
Aggregate Type:	Grn/Sand/RAP/RAS
Design Gradation Type:	DGA

Avg. Lab Properties of Plant Produced Mix

Sieve Size	Target	QC
25 mm (1"):	100	100
19 mm (3/4"):	100	100
12.5 mm (1/2"):	100	99
9.5 mm (3/8"):	99	98
4.75 mm (#4):	70	66
2.36 mm (#8):	45	51
1.18 mm (#16):	35	41
0.60 mm (#30):	23	30
0.30 mm (#50):	14	17
0.15 mm (#100):	9	11
0.075 mm (#200):	6.1	7.1
Binder Content (Pb):	5.5	5.3
Eff. Binder Content (Pbe):	5.0	4.8
Dust-to-Eff. Binder Ratio:	1.2	1.5
RAP Binder Replacement (%):	19.9	18.0
RAS Binder Replacement (%):	15.9	19.2
Total Binder Replacement (%):	35.8	37.2
Rice Gravity (Gmm):	2.483	2.492
Bulk Gravity (Gmb):	2.383	2.415
Air Voids (Va):	4.0	3.1
Agg. Bulk Gravity (Gsb):	2.668	2.67
VMA:	15.5	14
VFA:	74	79

Construction Diary

Relevant Conditions for Construction

Completion Date:	July 29, 2015
24 Hour High Temperature (F):	96
24 Hour Low Temperature (F):	74
24 Hour Rainfall (in):	0.07
Planned Subot Lift Thickness (in):	1.5
Paving Machine:	Roadtec

Plant Configuration and Placement Details

Component	% Setting
Binder Content (Plant Setting)	5.0
89 Granite	42.0
Coarse Sand	22.0
M10 Granite	11.0
EAP -1/2 RAP	20.0
EAP Post Consumer RAS	5.0
Evotherm P15	0.5

As-Built Sublot Lift Thickness (in):	1.5
Total Thickness of All New Sublots (in):	6.4
Approx. Underlying HMA Thickness (in):	4.9
Type of Tack Coat Utilized:	NTSS-1HM
Undiluted Target Tack Rate (gal/sy):	0.10
Approx. Avg. Temperature at Plant (F):	315
Avg. Measured Mat Compaction:	91.5%

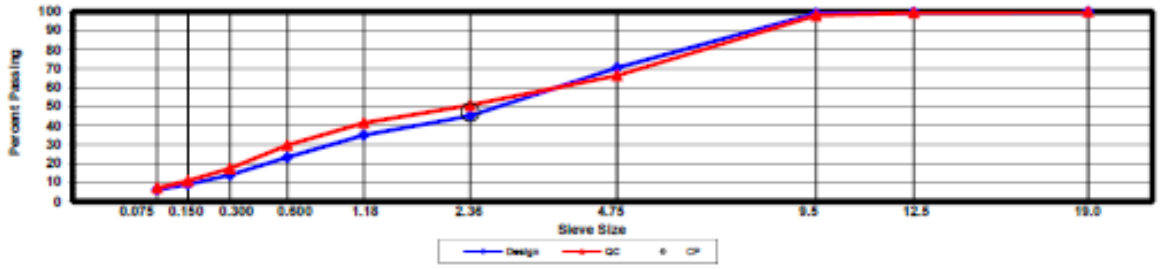

General Notes:
- References are by quadrant (E=East, N=North, W=West, S=South, L=Lee Rd 159, U=US-280), section #, and sublot (top=1).
- DGA, SMA, & OGFC refer to dense graded asphalt, stone matrix asphalt, & open-graded friction course, respectively.
- Production Gsb estimated using the actual production Gse and the difference between Gse and Gsb in the mix design.

Section and/or Sublot Specific Notes:
A significant amount of additional rubber tired rolling was required in order to get the density of this mat to an acceptable level.

5/23/2016

Quadrant: S
Section: 5
Sublot: 1

Laboratory Diary

General Description of Mix and Materials

Design Method:	Superpave
Compactive Effort:	80 gyrations
Binder Performance Grade:	58-28
Modifier Type:	SBS
Aggregate Type:	Granite/Sand/RAP
Design Gradation Type:	DGA

Avg. Lab Properties of Plant Produced Mix

Sieve Size	Target	QC
25 mm (1"):	100	100
19 mm (3/4"):	100	100
12.5 mm (1/2"):	100	99
9.5 mm (3/8"):	98	96
4.75 mm (#4):	74	73
2.36 mm (#8):	52	56
1.18 mm (#16):	41	44
0.60 mm (#30):	27	29
0.30 mm (#50):	15	16
0.15 mm (#100):	10	10
0.075 mm (#200):	6.3	6.3
Binder Content (Pb):	5.7	5.8
Eff. Binder Content (Pbe):	5.0	5.1
Dust-to-Eff. Binder Ratio:	1.2	1.2
RAP Binder Replacement (%):	33.5	29.2
RAS Binder Replacement (%):	0.0	0.0
Total Binder Replacement (%):	33.5	29.2
Rice Gravity (Gmm):	2.481	2.472
Bulk Gravity (Gmb):	2.382	2.393
Air Voids (Va):	4.0	3.2
Agg. Bulk Gravity (Gsb):	2.665	2.66
VMA:	15.7	15
VFA:	75	79

Construction Diary

Relevant Conditions for Construction

Completion Date:	July 23, 2015
24 Hour High Temperature (F):	92
24 Hour Low Temperature (F):	72
24 Hour Rainfall (in):	1.06
Planned Subot Lift Thickness (in):	1.5
Paving Machine:	Roadtec

Plant Configuration and Placement Details

Component	% Setting
Binder Content (Plant Setting)	5.6
89 Granite	30.0
Coarse Sand	24.0
M10 Granite	11.0
EAP -1/2 RAP	35.0
Evotherm P15	0.5

As-Built Sublot Lift Thickness (in):	1.6
Total Thickness of All New Sublots (in):	6.4
Approx. Underlying HMA Thickness (in):	4.8
Type of Tack Coat Utilized:	NTSS-1HM
Undilluted Target Tack Rate (gal/sy):	0.10
Approx. Avg. Temperature at Plant (F):	340
Avg. Measured Mat Compaction:	92.2%

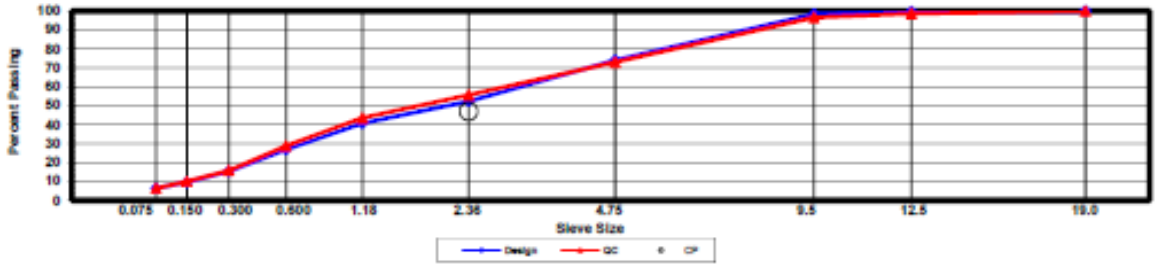

General Notes:
- References are by quadrant (E=East, N=North, W=West, S=South, L=Lee Rd 159, U=US-280), section #, and sublot (top=1).
- DGA, SMA, & OGFC refer to dense graded asphalt, stone matrix asphalt, & open-graded friction course, respectively.
- Production Gsb estimated using the actual production Gse and the difference between Gse and Gsb in the mix design.

Section and/or Sublot Specific Notes:
NA

5/23/2016

Quadrant: S
Section: 6
Sublot: 1

Laboratory Diary

General Descciption of Mix and Materials

Design Method:	Super
Compactive Effort:	80 gyrations
Binder Performance Grade:	HMA
Modifier Type:	Kraton
Aggregate Type:	Granite/Sand/RAP
Design Gradation Type:	DGA

Avg. Lab Properties of Plant Produced Mix

Sieve Size	Target	QC
25 mm (1"):	100	100
19 mm (3/4"):	100	100
12.5 mm (1/2"):	100	100
9.5 mm (3/8"):	99	98
4.75 mm (#4):	74	67
2.36 mm (#8):	51	52
1.18 mm (#16):	39	42
0.60 mm (#30):	26	28
0.30 mm (#50):	15	15
0.15 mm (#100):	9	9
0.075 mm (#200):	6.2	5.4
Binder Content (Pb):	5.9	5.8
Eff. Binder Content (Pbe):	5.2	5.0
Dust-to-Eff. Binder Ratio:	1.2	1.1
RAP Binder Replacement (%):	18.4	16.6
RAS Binder Replacement (%):	0.0	0.0
Total Binder Replacement (%):	18.4	16.6
Rice Gravity (Gmm):	2.470	2.459
Bulk Gravity (Gmb):	2.371	2.384
Air Voids (Va):	4.0	3.1
Agg. Bulk Gravity (Gsb):	2.654	2.63
VMA:	16.0	15
VFA:	75	79

Construction Diary

Relevant Conditions for Construction

Completion Date:	July 28, 2015
24 Hour High Temperature (F):	97
24 Hour Low Temperature (F):	74
24 Hour Rainfall (in):	0.00
Planned Subot Lift Thickness (in):	1.5
Paving Machine:	Roadtec

Plant Configuration and Placement Details

Component	% Setting
Binder Content (Plant Setting)	5.8
89 Granite	39.0
Coarse Sand	25.0
M10 Granite	16.0
EAP -1/2 RAP	20.0
Evotherm P15	0.5
As-Built Sublot Lift Thickness (in):	1.5
Total Thickness of All New Sublots (in):	6.5
Approx. Underlying HMA Thickness (in):	5.0
Type of Tack Coat Utilized:	NTSS-1HM
Undilluted Target Tack Rate (gal/sy):	0.10
Approx. Avg. Temperature at Plant (F):	340
Avg. Measured Mat Compaction:	91.8%

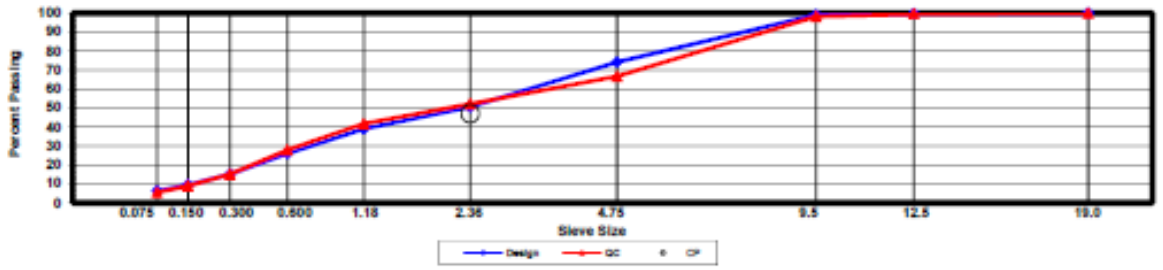

General Notes:
- References are by quadrant (E=East, N=North, W=West, S=South, L=Lee Rd 159, U=US-280), section #, and sublot (top=1).
- DGA, SMA, & OGFC refer to dense graded asphalt, stone matrix asphalt, & open-graded friction course, respectively.
- Production Gsb estimated using the actual production Gse and the difference between Gse and Gsb in the mix design.

Section and/or Sublot Specific Notes:
NA

5/23/2016

Quadrant: S
Section: 13
Sublot: 1

Laboratory Diary

General Description of Mix and Materials

Design Method:	AZ
Compactive Effort:	75 blows
Binder Performance Grade:	ARB20
Modifier Type:	GTR
Aggregate Type:	Granite/Sand/C-RAP
Design Gradation Type:	GAP

Avg. Lab Properties of Plant Produced Mix

Sieve Size	Target	QC
25 mm (1"):	100	100
19 mm (3/4"):	100	100
12.5 mm (1/2"):	96	96
9.5 mm (3/8"):	79	85
4.75 mm (#4):	40	35
2.36 mm (#8):	24	22
1.18 mm (#16):	19	19
0.60 mm (#30):	12	14
0.30 mm (#50):	7	8
0.15 mm (#100):	5	5
0.075 mm (#200):	3.4	3.6
Binder Content (Pb):	7.4	7.4
Eff. Binder Content (Pbe):	6.7	6.7
Dust-to-Eff. Binder Ratio:	0.6	0.5
RAP Binder Replacement (%):	7.5	7.5
RAS Binder Replacement (%):	0.0	0.0
Total Binder Replacement (%):	7.5	7.5
Rice Gravity (Gmm):	2.418	2.402
Bulk Gravity (Gmb):	2.273	2.319
Air Voids (Va):	6.0	3.4
Agg. Bulk Gravity (Gsb):	2.649	2.63
VMA:	19.9	18
VFA:	71	81

Construction Diary

Relevant Conditions for Construction

Completion Date:	August 14, 2015
24 Hour High Temperature (F):	91
24 Hour Low Temperature (F):	73
24 Hour Rainfall (in):	0.00
Planned Subot Lift Thickness (in):	1.5
Paving Machine:	Roadtec

Plant Configuration and Placement Details

Component	% Setting
Binder Content (Plant Setting)	7.4
78 Granite	55.0
89 Granite	19.0
Coarse Sand	11.0
EAP Coarse RAP	15.0
Evotherm P15	0.5

As-Built Sublot Lift Thickness (in):	1.6
Total Thickness of All New Sublots (in):	6.7
Approx. Underlying HMA Thickness (in):	5.0
Type of Tack Coat Utilized:	NTSS-1HM
Undiluted Target Tack Rate (gal/sy):	0.10
Approx. Avg. Temperature at Plant (F):	305
Avg. Measured Mat Compaction:	92.7%

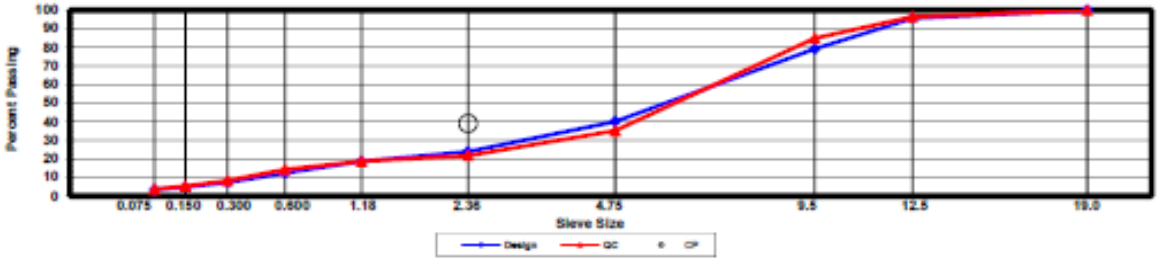

General Notes:
- References are by quadrant (E=East, N=North, W=West, S=South, L=Lee Rd 159, U=US-280), section #, and sublot (top=1).
- DGA, SMA, & OGFC refer to dense graded asphalt, stone matrix asphalt, & open-graded friction course, respectively.
- Production Gsb estimated using the actual production Gse and the difference between Gse and Gsb in the mix design.

Section and/or Sublot Specific Notes:
Binder for this surface mix contained 20% (by total binder mass) -#16 mesh ground tire rubber to build on the success of the base layer in S13 on the 2012 Track, this time in a surface mix application at the request of ALDOT in order to support implementation of the new mix technology.

APPENDIX B – CRACKING TEST RESULTS

Energy Ratio Testing Results

Mixture ID	*Creep Compliance*			*Resilient Modulus*	*Indirect Tension*		
	m-value	*D_1*	*Compliance Rate*	*M_r (GPa)*	*S_t (MPa)*	*FE (kJ/m^3)*	*Failure Strain*
N1 - 20% RAP Ctrl	0.407	5.582E-07	3.79E-09	9.94	2.37	4.80	2,584
N2 - High Dens Ctrl	0.375	3.956E-07	1.98E-09	12.41	2.83	3.90	1,894
N5 - Low AC & Dens Ctrl	0.396	7.076E-07	4.31E-09	7.93	1.82	3.40	2,349
N8 - Ctrl + 5% RAS	0.252	3.475E-07	4.98E-10	12.75	2.42	1.80	1,047
S5 - 35% RAP w/ 58-28	0.347	9.102E-07	3.46E-09	7.38	1.87	6.00	3,840
S6 - Ctrl w/ HiMA	0.313	8.966E-07	2.44E-09	7.28	1.81	5.40	3,953
S13 - 15% RAP AZ GTR	0.351	1.302E-06	5.17E-09	7.40	1.62	2.70	2,208

Mixture ID	*Target V_a (%)*	*Stress (psi)*	*a*	*$DCSE_{HMA}$ (kJ/m^3)*	*$DCSE_{Min}$ (kJ/m^3)*	*ER*
N1 - 20% RAP Ctrl	7	150	4.68E-08	4.52	0.82	5.52
N2 - High Dens Ctrl	4	150	4.43E-08	3.58	0.48	7.43
N5 - Low AC & Dens Ctrl	10	150	4.99E-08	3.19	0.89	3.57
N8 - Ctrl + 5% RAS	7	150	4.66E-08	1.57	0.12	12.82
S5 - 35% RAP w/ 58-28	7	150	4.96E-08	5.76	0.78	7.39
S6 - Ctrl w/ HiMA	7	150	5.00E-08	5.17	0.56	9.18
S13 - 15% RAP AZ GTR	7	150	5.10E-08	2.52	1.13	2.24

TX Overlay Testing Results

Mixture ID	*Sample ID*	*Va (%)*	*Temp (°C)*	*MOD (in)*	*Frequency*	N_f
N1 - 20% RAP Ctrl	#1B	6.8	25	0.635	0.1	32
N1 - 20% RAP Ctrl	#2A	7.0	25	0.635	0.1	10
N1 - 20% RAP Ctrl	#3B	7.0	25	0.635	0.1	49
N1 - 20% RAP Ctrl	#4A	7.2	25	0.635	0.1	8
N2 - High Dens Ctrl	#2B	3.9	25	0.635	0.1	24
N2 - High Dens Ctrl	#3A	3.9	25	0.635	0.1	17
N2 - High Dens Ctrl	#4A	4.2	25	0.635	0.1	112
N2 - High Dens Ctrl	#5A	4.0	25	0.635	0.1	82
N5 - Low AC & Dens Ctrl	#1B	9.8	25	0.635	0.1	23
N5 - Low AC & Dens Ctrl	#2A	10.2	25	0.635	0.1	13
N5 - Low AC & Dens Ctrl	#3B	10.0	25	0.635	0.1	15
N5 - Low AC & Dens Ctrl	#4B	10.3	25	0.635	0.1	18
N8 - Ctrl + 5% RAS	#1B	6.7	25	0.635	0.1	2
N8 - Ctrl + 5% RAS	#2A	6.3	25	0.635	0.1	2
N8 - Ctrl + 5% RAS	#3A	6.5	25	0.635	0.1	2
N8 - Ctrl + 5% RAS	#4B	6.6	25	0.635	0.1	2
S5 - 35% RAP w/ 58-28	#1A	7.3	25	0.635	0.1	37
S5 - 35% RAP w/ 58-28	#2A	7.4	25	0.635	0.1	73
S5 - 35% RAP w/ 58-28	#1B	7.0	25	0.635	0.1	110
S5 - 35% RAP w/ 58-28	#6B	7.3	25	0.635	0.1	23
S6 - Ctrl w/ HiMA	#1B	6.4	25	0.635	0.1	15
S6 - Ctrl w/ HiMA	#3A	6.4	25	0.635	0.1	6
S6 - Ctrl w/ HiMA	#5A	6.4	25	0.635	0.1	18
S13 - 15% RAP AZ GTR	#1A	7.1	25	0.635	0.1	1519
S13 - 15% RAP AZ GTR	#2A	6.8	25	0.635	0.1	1857
S13 - 15% RAP AZ GTR	#3B	7.1	25	0.635	0.1	2166
S13 - 15% RAP AZ GTR	#6B	6.6	25	0.635	0.1	1358

NCAT Overlay Testing Results

Mixture ID	*Sample ID*	*Va (%)*	*Temp (°C)*	*MOD (in)*	*Frequency*	*Nf*
N1 - 20% RAP Ctrl	#1A	7.2	25	0.381	1	342
N1 - 20% RAP Ctrl	#2B	6.7	25	0.381	1	452
N1 - 20% RAP Ctrl	#3A	7.0	25	0.381	1	607
N1 - 20% RAP Ctrl	#5A	6.8	25	0.381	1	662
N2 - High Dens Ctrl	#2A	3.9	25	0.381	1	762
N2 - High Dens Ctrl	#3B	4.0	25	0.381	1	600
N2 - High Dens Ctrl	#4B	3.7	25	0.381	1	318
N2 - High Dens Ctrl	#5B	3.8	25	0.381	1	1109
N5 - Low AC & Dens Ctrl	#1A	10.3	25	0.381	1	235
N5 - Low AC & Dens Ctrl	#2B	10.0	25	0.381	1	179
N5 - Low AC & Dens Ctrl	#3A	10.3	25	0.381	1	121
N5 - Low AC & Dens Ctrl	#4A	10.3	25	0.381	1	219
N8 - Ctrl + 5% RAS	#1A	6.8	25	0.381	1	14
N8 - Ctrl + 5% RAS	#2B	6.8	25	0.381	1	10
N8 - Ctrl + 5% RAS	#3B	6.5	25	0.381	1	13
S5 - 35% RAP w/ 58-28	#2B	7.2	25	0.381	1	586
S5 - 35% RAP w/ 58-28	#4A	7.5	25	0.381	1	1037
S5 - 35% RAP w/ 58-28	#6A	6.9	25	0.381	1	697
S6 - Ctrl w/ HiMA	#2B	6.5	25	0.381	1	211
S6 - Ctrl w/ HiMA	#3B	6.3	25	0.381	1	728
S6 - Ctrl w/ HiMA	#4B	6.2	25	0.381	1	294
S13 - 15% RAP AZ GTR	#1B	6.6	25	0.381	1	2188
S13 - 15% RAP AZ GTR	#3A	6.7	25	0.381	1	4072
S13 - 15% RAP AZ GTR	#5A	7.3	25	0.381	1	2902

Semi-Circular Bend Testing Results

Mixture ID	*Sample ID*	*Air Voids (%)*	*Notch Length (mm)*	*Ligament Length (mm)*	*Peak Load (KN)*	*Disp. @ Peak Load (mm)*	*Strain Energy @ Peak Load (KN-mm)*
N1 - 20% RAP Ctrl	8A-1	7.1	24.75	48.75	1.017	0.832	0.500
N1 - 20% RAP Ctrl	9A-1	7.0	24.90	48.40	0.971	0.937	0.586
N1 - 20% RAP Ctrl	9B-1	6.9	25.85	48.20	1.050	0.861	0.573
N1 - 20% RAP Ctrl	10A-1	6.9	24.95	48.65	0.930	0.795	0.477
N1 - 20% RAP Ctrl	2A-2	7.2	31.65	41.65	0.783	0.879	0.465
N1 - 20% RAP Ctrl	2B-2	7.2	32.80	41.50	0.787	0.773	0.385
N1 - 20% RAP Ctrl	3A-2	6.9	31.40	42.40	0.807	0.685	0.341
N1 - 20% RAP Ctrl	3B-2	7.2	32.30	41.75	0.882	0.707	0.390
N1 - 20% RAP Ctrl	4B-3	6.8	38.20	35.60	0.536	0.756	0.273
N1 - 20% RAP Ctrl	5A-3	7.3	37.30	36.10	0.537	0.710	0.239
N1 - 20% RAP Ctrl	5B-3	7.1	38.05	35.85	0.565	0.776	0.280
N2 - High Dens Ctrl	4A-1	4.0	25.10	48.50	1.494	0.893	0.771
N2 - High Dens Ctrl	4B-1	3.9	25.10	48.95	1.430	0.847	0.739
N2 - High Dens Ctrl	7A-1	3.8	24.80	48.70	1.578	0.794	0.762
N2 - High Dens Ctrl	5A-2	4.1	31.45	42.05	1.084	0.701	0.470
N2 - High Dens Ctrl	5B-2	4.0	32.50	41.65	1.182	0.747	0.515
N2 - High Dens Ctrl	6A-2	3.9	31.80	41.85	1.128	0.698	0.488
N2 - High Dens Ctrl	3A-3	3.7	37.40	36.10	0.849	0.575	0.298
N2 - High Dens Ctrl	3B-3	3.9	38.20	35.50	0.930	0.594	0.333
N2 - High Dens Ctrl	8A-3	4.0	37.25	36.50	0.781	0.603	0.289
N2 - High Dens Ctrl	8B-3	4.0	37.30	36.30	0.863	0.663	0.348
N5 - Low AC & Dens Ctrl	2B-1	10.1	25.20	49.05	0.797	0.773	0.377
N5 - Low AC & Dens Ctrl	5A-1	9.5	24.85	48.50	0.856	0.818	0.464
N5 - Low AC & Dens Ctrl	5B-1	9.8	25.25	49.10	0.950	0.882	0.543
N5 - Low AC & Dens Ctrl	6A-1	9.7	24.65	48.65	0.951	0.818	0.467
N5 - Low AC & Dens Ctrl	4A-2	10.2	31.80	41.75	0.575	0.783	0.276
N5 - Low AC & Dens Ctrl	4B-2	9.9	32.55	41.65	0.597	0.810	0.321
N5 - Low AC & Dens Ctrl	7A-2	9.9	32.80	41.45	0.651	0.699	0.289
N5 - Low AC & Dens Ctrl	8B-2	9.9	31.75	41.60	0.624	0.657	0.249
N5 - Low AC & Dens Ctrl	1A-3	9.6	37.60	36.85	0.488	0.811	0.268
N5 - Low AC & Dens Ctrl	3B-3	9.7	38.00	36.10	0.497	0.692	0.214
N5 - Low AC & Dens Ctrl	10A-3	9.9	37.35	36.15	0.479	0.583	0.168
N5 - Low AC & Dens Ctrl	10B-3	9.9	37.95	36.30	0.490	0.669	0.221

Mixture ID	*Sample ID*	*Air Voids (%)*	*Notch Length (mm)*	*Ligament Length (mm)*	*Peak Load (KN)*	*Disp. @ Peak Load (mm)*	*Strain Energy @ Peak Load (KN-mm)*
N8 - Ctrl + 5% RAS	3B-1	6.5	25.45	48.75	1.700	0.466	0.409
N8 - Ctrl + 5% RAS	8A-1	6.9	24.75	48.80	1.658	0.512	0.457
N8 - Ctrl + 5% RAS	8B-1	6.7	25.05	49.05	1.350	0.628	0.551
N8 - Ctrl + 5% RAS	10A-1	7.1	24.50	48.75	1.750	0.516	0.469
N8 - Ctrl + 5% RAS	5B-2	7.0	31.70	41.80	1.175	0.498	0.279
N8 - Ctrl + 5% RAS	9A-2	7.3	32.60	41.80	1.078	0.472	0.285
N8 - Ctrl + 5% RAS	9B-2	6.9	31.50	41.95	1.221	0.477	0.282
N8 - Ctrl + 5% RAS	2A-3	7.1	38.05	36.00	1.046	0.411	0.199
N8 - Ctrl + 5% RAS	4A-3	6.9	37.65	36.15	1.031	0.399	0.208
N8 - Ctrl + 5% RAS	7A-3	7.1	37.60	36.55	0.980	0.354	0.176
N8 - Ctrl + 5% RAS	7B-3	7.0	37.10	36.25	1.143	0.394	0.196
S5 - 35% RAP w/ 58-28	3A-1	7.0	25.60	48.08	0.731	0.966	0.413
S5 - 35% RAP w/ 58-28	3B-1	6.8	26.08	48.03	0.735	1.125	0.547
S5 - 35% RAP w/ 58-28	4A-1	6.9	25.34	48.16	0.673	1.041	0.446
S5 - 35% RAP w/ 58-28	4B-1	6.8	25.97	48.14	0.654	1.139	0.481
S5 - 35% RAP w/ 58-28	6A-2	6.9	31.78	42.16	0.519	0.973	0.332
S5 - 35% RAP w/ 58-28	6B-2	7.1	31.10	42.55	0.481	0.940	0.291
S5 - 35% RAP w/ 58-28	9A-2	7.1	31.44	42.29	0.491	1.054	0.353
S5 - 35% RAP w/ 58-28	9B-2	7.0	31.65	42.30	0.585	0.928	0.329
S5 - 35% RAP w/ 58-28	2B-3	7.1	38.24	35.75	0.416	0.857	0.235
S5 - 35% RAP w/ 58-28	7A-3	6.9	37.52	36.15	0.397	0.812	0.189
S5 - 35% RAP w/ 58-28	7B-3	7.0	37.93	36.05	0.372	1.094	0.283
S5 - 35% RAP w/ 58-28	10A-3	7.1	37.77	35.91	0.428	0.835	0.229
S6 - Ctrl w/ HiMA	1B-1	7.0	26.04	47.99	0.798	0.897	0.459
S6 - Ctrl w/ HiMA	4A-1	6.8	25.62	47.96	0.867	0.910	0.508
S6 - Ctrl w/ HiMA	4B-1	6.9	26.15	47.87	0.857	0.916	0.479
S6 - Ctrl w/ HiMA	7A-1	6.8	25.52	48.13	0.937	0.863	0.507
S6 - Ctrl w/ HiMA	3A-2	6.9	32.77	41.34	0.753	0.719	0.319
S6 - Ctrl w/ HiMA	3B-2	6.8	31.70	41.72	0.770	0.837	0.374
S6 - Ctrl w/ HiMA	6B-2	7.1	31.86	42.16	0.698	0.718	0.315
S6 - Ctrl w/ HiMA	8A-2	6.9	31.91	42.14	0.658	0.845	0.363
S6 - Ctrl w/ HiMA	2A-3	6.8	37.57	36.02	0.526	0.674	0.226
S6 - Ctrl w/ HiMA	2B-3	6.9	38.36	35.50	0.472	0.799	0.247
S6 - Ctrl w/ HiMA	9B-3	6.9	38.02	36.08	0.456	0.798	0.218
S6 - Ctrl w/ HiMA	10B-3	7.1	38.15	35.61	0.488	0.719	0.241

Mixture ID	*Sample ID*	*Air Voids (%)*	*Notch Length (mm)*	*Ligament Length (mm)*	*Peak Load (KN)*	*Disp. @ Peak Load (mm)*	*Strain Energy @ Peak Load (KN-mm)*
S13 - 15% RAP AZ GTR	1B-1	7.2	25.77	47.84	0.854	1.483	0.838
S13 - 15% RAP AZ GTR	8A-1	7.1	25.44	47.84	0.855	1.383	0.801
S13 - 15% RAP AZ GTR	10B-1	7.2	26.00	47.73	0.880	1.338	0.803
S13 - 15% RAP AZ GTR	BA-2	7.5	31.89	41.85	0.550	1.476	0.582
S13 - 15% RAP AZ GTR	6A-2	7.4	31.41	42.18	0.592	1.781	0.725
S13 - 15% RAP AZ GTR	9B-2	7.4	31.88	41.91	0.683	1.479	0.679
S13 - 15% RAP AZ GTR	10A-2	7.4	31.91	41.18	0.612	1.110	0.438
S13 - 15% RAP AZ GTR	3A-3	7.3	37.83	35.56	0.479	1.495	0.517
S13 - 15% RAP AZ GTR	4A-3	7.6	37.71	35.57	0.398	1.333	0.387
S13 - 15% RAP AZ GTR	4B-3	7.0	38.21	35.39	0.447	1.439	0.464
S13 - 15% RAP AZ GTR	7A-3	7.3	37.60	36.05	0.424	1.542	0.464

Illinois Flexibility Index Testing Results

Mixture ID	*Sample ID*	*Air Voids (%)*	*Peak Load (kN)*	*Slope (kN/mm)*	*Fracture Energy (J/m^2)*	*Flexibility Index (FI)*	*Strength (psi)*
N1 - 20% RAP Ctrl	1A	7.1	3.46	-4.56	1509	3.31	65.8
N1 - 20% RAP Ctrl	2A	7.3	3.36	-4.18	1481	3.54	65.0
N1 - 20% RAP Ctrl	2B	7.4	3.55	-4.13	1597	3.87	69.0
N1 - 20% RAP Ctrl	2C	7.4	3.43	-3.93	1553	3.95	66.4
N1 - 20% RAP Ctrl	3A	7.0	3.60	-4.21	1607	3.82	69.4
N1 - 20% RAP Ctrl	3B	7.5	3.73	-4.66	1582	3.39	72.5
N1 - 20% RAP Ctrl	4D	7.4	3.36	-4.45	1422	3.20	64.3
N2 - High Dens Ctrl	1B	4.4	5.43	-11.23	1620	1.44	102.9
N2 - High Dens Ctrl	1D	4.6	5.27	-8.82	1796	2.04	99.2
N2 - High Dens Ctrl	2C	4.9	4.88	-8.27	1630	1.97	93.7
N2 - High Dens Ctrl	3A	4.5	4.81	-7.79	1546	1.98	91.8
N2 - High Dens Ctrl	3C	4.4	5.14	-8.90	1652	1.86	97.3
N5 - Low AC & Dens Ctrl	2A	10.0	3.09	-3.91	1149	2.94	59.2
N5 - Low AC & Dens Ctrl	2B	10.3	3.10	-5.50	1172	2.13	59.1
N5 - Low AC & Dens Ctrl	2D	10.5	3.06	-4.44	1242	2.80	58.4
N5 - Low AC & Dens Ctrl	3A	10.5	3.15	-5.17	117	2.16	60.5
N5 - Low AC & Dens Ctrl	3B	10.3	3.01	-3.23	1311	4.06	57.6
N5 - Low AC & Dens Ctrl	5A	10.4	2.83	-4.94	1017	2.06	53.5
N8 - Ctrl + 5% RAS	1B	7.0	5.21	-30.39	1025	0.34	99.4
N8 - Ctrl + 5% RAS	1D	7.1	4.93	-18.77	947	0.50	94.2
N8 - Ctrl + 5% RAS	2B	6.7	5.66	-29.51	999	0.34	107.5
N8 - Ctrl + 5% RAS	2C	7.0	5.11	-25.68	980	0.38	98.1
N8 - Ctrl + 5% RAS	2D	6.7	5.66	-27.34	964	0.35	108.3
N8 - Ctrl + 5% RAS	4A	6.8	4.80	-18.99	851	0.45	91.4
N8 - Ctrl + 5% RAS	4B	6.8	5.17	-21.72	1062	0.49	98.5
N8 - Ctrl + 5% RAS	4C	7.0	5.09	-27.44	931	0.34	97.9
N8 - Ctrl + 5% RAS	4D	6.9	5.35	-29.27	906	0.31	102.8
S6 - Ctrl w/ HiMA	1A	6.9	3.17	-3.50	1509	4.31	61.0
S6 - Ctrl w/ HiMA	1B	7.4	3.31	-3.41	1476	4.33	63.3
S6 - Ctrl w/ HiMA	1D	7.0	3.08	-3.03	1512	4.99	59.4
S6 - Ctrl w/ HiMA	2B	7.3	3.48	-3.52	1613	4.58	66.2
S6 - Ctrl w/ HiMA	3B	7.4	3.08	-3.47	1544	4.45	58.5
S5 - 35% RAP w/ 58-28	1A	7.6	3.01	-2.65	1549	5.85	57.3
S5 - 35% RAP w/ 58-28	2C	7.3	2.65	-2.31	1473	6.38	52.0
S5 - 35% RAP w/ 58-28	2D	6.8	2.41	-2.04	1389	6.81	48.0
S5 - 35% RAP w/ 58-28	4A	7.2	2.60	-2.27	1463	6.45	49.6
S5 - 35% RAP w/ 58-28	4B	7.0	2.77	-2.72	1412	5.19	53.3
S5 - 35% RAP w/ 58-28	4D	7.6	2.63	-2.21	1527	6.91	50.8

Mixture ID	*Sample ID*	*Air Voids (%)*	*Peak Load (kN)*	*Slope (kN/mm)*	*Fracture Energy (J/m^2)*	*Flexibility Index (FI)*	*Strength (psi)*
S13 - 15% RAP AZ GTR	1A	7.0	3.15	-1.91	2493	13.05	61.5
S13 - 15% RAP AZ GTR	1B	7.6	3.88	-2.01	2676	13.31	60.1
S13 - 15% RAP AZ GTR	2C	7.0	3.54	-3.11	2191	7.04	67.6
S13 - 15% RAP AZ GTR	2D	7.5	2.99	-1.55	2540	16.38	57.1
S13 - 15% RAP AZ GTR	4B	6.5	3.81	-3.76	2108	5.61	72.4
S13 - 15% RAP AZ GTR	4C	6.6	3.41	-2.61	1828	7.00	65.4